UNIVERSIDAD DE ANTIOQUIA

A Multi-Period Model for the Optimal Reactive Power Dispatch Problem

Jairo Arturo Morán Burgos

Tesis de maestría presentada para optar al título de Magíster en Ingeniería

Director
Jesús M. López-Lezama, Doctor (PhD)
Codirector
Walter M. Villa-Acevedo, Magíster (MSc)

Universidad de Antioquia
Facultad de Ingeniería
Maestría en Ingeniería
Medellín, Antioquia, Colombia
2022

Cita		Morán-Burgos [1]
Referencia Estilo IEEE (2020)	[1]	J. A. Morán-Burgos, "A Multi-Period Model for the Optimal Reactive Power Dispatch Problem", Tesis de maestría, Maestría en Ingeniería, Universidad de Antioquia, Medellín, Antioquia, Colombia, 2022.

Maestría en Ingeniería, Energética.

Grupo de Investigación Manejo Eficiente de la Energía (GIMEL).

Sede de Investigación Universitaria (SIU).

"If I have seen further, it is by standing on the shoulders of giants"

Issac Newton

Abstract

The optimal reactive power dispatch (ORPD) problem plays a key role in daily power system operation. This thesis presents a novel multi-period approach for the ORPD that takes into account three operative goals. These consist on minimizing total voltage deviations from set point values of pilot nodes as well as maneuvers on transformers taps and reactive power compensators. The ORPD is formulated in GAMS (General Algebraic Modeling System) software as a mixed integer nonlinear programming problem, comprising both continuous and discrete control variables and solved using BONMIN (Basic Open-source Nonlinear Mixed INteger programming) solver. The most outstanding benefits of the proposed ORPD model is the fact that it allows an optimal reactive power control throughout a multi-period horizon, guaranteeing compliance with the programmed active power dispatch. Also, the minimization of maneuvers on reactors and capacitor banks contributes to preserving the useful life of these devices. Furthermore, the selection of pilot nodes for voltage control reduces computational burden and allows the algorithm to provide fast solutions. Results on the IEEE 57 and IEEE 118 bus test systems evidenced the applicability and effectiveness of the proposed approach.

Acknowledgements

First and foremost, I thank God who is the pillar of my life and whatever good thing I do is in his name.

I would like to express my sincere gratitude to my advisor, Professor Jesús María López Lezama from Universidad de Antioquia, for his much-valued guidance, suggestions, patience, and encouragement throughout this work. I would also like to thank my co-advisor, Professor Walter Mauricio Villa, his pertinent corrections, enthusiasm, guide to do things in a practical and simple way.

I was fortunate to meet good friends which motivated and inspired me with their example and words to be integral. Part of this thesis was completed thanks to Juan Sierra, who helped me to understand the optimization models and was willing to support me at any time. My thanks, also, to Jorge Urrea, Wilmer Ropero, Brigitte Roldán, Ricardo Pardo and Jorge Esteban, my colleagues and friends, who were always generous in sharing their thoughts and broad knowledge.

Thanks to María Elena who has been always with me, and being my best friend. This thesis is in her honor.

Contents

Chapter 1

Motivation and objectives

1.1 Introduction

The management of voltages and reactive power in large power systems are of great relevance today, both at the planning and operating levels [1]. This problem has become very critical in the last decade due to the lack of reactive power resources together with the increase in demand and with it the increase in the needs for this power. Some aspects that have contributed to this lack of investment in resources are the increase in energy costs, the demands for a higher quality of service and the need to make better use of existing facilities [2].

The supply of reactive power to the grid is a very important issue in the power systems operation. The independent system operator (ISO) is in charge of managing the reactive power resources available. Such resources include generators, capacitors, reactors, transformers, VQ controls, SVCs, STATCOMs, lines, etc. [3].

In some systems the voltage regulation is carried out automatically, supported by pilot nodes and voltage control areas [4,5], examples include France [6] and Italy [7] with 35 and 18 pilot nodes, respectively. This option has become very attractive for the ISO, because in radial areas it simplifies and improves the voltage control, where the dv/dq is easily known. However, current systems are increasingly meshed and in higher demand. This makes the task of establishing voltage control areas difficult, as they may not be sufficiently decoupled, resulting in significantly adverse interactions, making automatic secondary control difficult. Therefore, the voltage control is carried out manually by the ISO [6]. However, today it is unsatisfactory because it relays on the operator's experience, offline predictions and operating conditions, which can often be different from those estimated. Operating a power system with large number of variables increases the difficulty of operating for the ISO. Therefore, a control based in optimization is necessary for a coordinate voltage control [8].

The optimal reactive power dispatch (ORPD) consists on finding a proper adjustment of reactive power resources whit the aim of minimizing an objective function. Therefore, it is a tool that is quite well suited to the problem of voltages control. However, classical model of ORPD is based on the principle of income maximization without considering costs of control actions [9]. Under real-time circumstances, this sort of solution is not practical because the number of control actions would be too large to be executed in actual power system operation [10]. Therefore, this new situation must be addressed, developing an ORPD model that takes into account: 1, the variation in demand, this to plan and make possible future actions. 2, the solution can be executed from the actual operation of the electrical power system, that is, the number of actions should not saturate the limit capacity of the system operator.

1.2 Main objective

To develop an optimal reactive power dispatch model that contemplates in its formulation: the multi-period analysis, the minimization of the voltage deviation in a set of

pilot nodes with respect to a reference, the number of maneuvers on the control devices and the network operating constraints.

1.3 Specific objectives

a. To carry out a specialized literature review of the current optimal reactive power dispatch models, which will be used as a basis for the construction of a multi-period model.
b. To build a mathematical model that takes into account within its constraints the number of maneuvers (transformers taps, shunt capacitors and rectors).
c. To implement the proposed mathematical model in an algebraic modeling language to solve the optimal reactive power dispatch.
d. To compare the performance of the objective value between the multi-period base case and the proposed formulation, to assess the adaptability of the proposal within the actual operation.

1.4 Thesis contributions

In this work, a mathematical model for the ORPD problem is developed from a multi-period approach considering multiple operative goals. The proposed formulation is presented as a MINLP problem. In this case, the maneuvers on shunt capacitors and reactors are considered as binary variables, while the voltage set-points of generation units as well as the transformer taps are modeled as continuous variables. However, the transformer taps are post-processed so that they have a discrete representation for the user. The model considers three operative goals composed in a weighted sum. In this way, the solution found can be adapted according to the requirements of the system operators. The first term refers to the voltage's deviation on a set of pilot nodes. The reference values may change in each period and represent safe values according to experience (the reference value is generally obtained from the historical average in each period and type of day). When the optimization is performed in a reduced set of total nodes, computation times are improved and voltage profiles can be adapted according to the areas controlled by each pilot node. The second term prevents excessive switching of shunt elements when the system does not require it, which implicitly reduces the number of maneuvers that are carried out and prevents the wear of these elements. The third term tries to conserve the dynamic reserve of reactive power on the power system; dynamic reserve is the capacity that generators must supply or absorb reactive power, proper margins of dynamic reserve allow a quick response against contingencies. Power flows are modeled through a polar power-voltage formulation (p-v), which is part of the set of Standard Line Power (SLP) models; p-v is the formulation that presents the best computational performance according to the bibliographic review. For the choice of pilot nodes, this thesis adopts the procedure introduced by [11], which is derived from the voltage stability analysis by dividing networks into control areas, so that the chosen nodes and their margins guarantee good operating points. The developed model is implemented in the IEEE-57 and IEEE-118 test systems with a 24-h demand curve for a typical spring weekday. This thesis presents a novel approach to solve the multiperiod- optimal reactive power dispatch (MP-ORPD) problem. The main features and contributions that differentiate this work from others reported in the specialized literature are as follows:

- The proposed MP-ORPD is envisaged from the point of view of a power system operator; in this case, a single objective function is not pursued as such; but instead, a set of goals regarding minimization of deviations from desired operational values are considered.

- The main goal of the MP-ORPD is guaranteeing operative feasibility throughout a given time horizon, while minimizing the number of maneuvers carried out in reactive power devices and transformers taps, preserving their useful life and therefore reducing eventual maintenance costs.
- Instead of considering all buses for enforcing voltage limits constraints, only a bunch of pilot nodes are taken into account. Furthermore, dynamic limits are considered in these buses to mimic real-life operation. This results in low computational effort which encourages real-life applications of the methodology.

1.5 Thesis outline

This work is organized as follows. Chapter 2 presents a literature review of the current context, provides the knowledge bases to understand the ORPD problem, the assumptions adopted, the solution methods and highlights the relevance of developing multi-period models for real power systems. Chapter 3 presents the proposed mathematical formulation (a full AC model under a MINLP approached). The model is broken down and explained in detail. Chapter 4 presents the tests and results carried out with two benchmark power systems: IEEE 57-bus and IEEE 118-bus test systems. The former is an approximation of a depleted electrical network, while the latter is a larger system that has all reactive control elements considered in the model. Chapter 5 presents general conclusions and several suggestions for future work.

1.6 List of publications

The following paper encompassing the whole thesis was published as the result of this research work:

- Morán-Burgos JA, Sierra-Aguilar JE, Villa-Acevedo WM, López-Lezama JM. A Multi-Period Optimal Reactive Power Dispatch Approach Considering Multiple Operative Goals. *Applied Sciences*. 2021; 11(18):8535. https://doi.org/10.3390/app11188535.

Chapter 2

Theoretical foundations and literature review

2.1 State of the art

The ORPD can be seen as an AC optimal power flow (OPF) problem with a particular set of control variables which include shunt compensations, transformer tap changers and voltage generator set-points. In this case, the active power output of all generators with the exception of the slack bus is kept constant [12]. The ORPD problem plays an important role in the economic and secure operation of power systems since it is one of the ways to face the problem of reactive power management and voltage control [13]. The main idea behind the ORPD problem is finding an optimal scheduling of the reactive power control devices within a network in such a way that operational constraints are met while also optimizing a given objective function [14]. A bunch of ORPD formulations and solution methods have been reported in the specialized literature to address specific instances of the problem [15]. These include different objective functions, controls, and system constraints, as well as distinct mathematical characteristics and computational requirements [16]. The resulting optimization problems go by many names depending on the particular objective function being addressed and the constraints under consideration [17,18].

The common feature of the literature methodologies is the fact they approach the static version of the ORPD problem [15,19,20]; that is to say, the optimization is carried out over a single time period. Real-life ORPD problems must consider a dynamic or multi-period approach and therefore are often significantly more challenging than the classically considered problems [8]. Under real-time circumstances, solutions provided by traditional ORPD models may not be practical because the number of control actions would be too large to be executed in actual power system operation [10]; furthermore, the computing time plays a key role in such applications. The MP-ORPD was originally proposed in [21] and in some papers is called dynamic ORPD (DORPD); its main focus is dealing with different loading conditions for a given future time interval instead of a single snapshot of the power network. The set of desirable features for real implementations of the MP-ORPD programs is extensive and can make the solution of the model a complex task. In this case, the control actions must be valid within a given time horizon, the improvement of voltage profile can be carried out resorting to pilot nodes and the number of control actions must not be excessive. A compilation of such features is presented in [22]. Compared with its traditional or static counterpart, the MP-ORPD is a more complex optimization problem having multiple local minima as well as nonlinear and discontinuous constraints [10].

The MP-ORPD is a hard problem to model and solve because its nature corresponds to a MINLP problem which involves both continuous and integer variables and whose objective function and feasible set are described by nonlinear functions [23]. Furthermore the intertemporal constrains for the maneuvers over control devices increase in problem complexity and computational time for its resolution, especially for large power systems [15]. In order to facilitate the ORPD solution, a number of efforts have been proposed for

handling discrete variables [12,24,25]. The simplest approach for handling discrete variables is based on the round-off strategy. In this technique, there are three steps: in the first step, the ORPD relaxation is solved by treating all variables as continuous. In the second step, at the optimal solution already found, the discrete variables are rounded-off to their nearest discrete value. In the third step, the discrete variables are frozen and the continuous variables are determined by re-solving the ORPD. Although it may lead to poor suboptimal solutions or infeasible ones. Some deficiencies were already pointed out in [26]: for instance, since the ORPD problem is in general highly nonconvex, solving its continuous relaxation with a local optimizer in the first step may lead to a poor local solution which, after round-off in the second step, may lead to a very poor solution in the third step.

There are relatively few studies that approach the dynamic or MP-ORPD. Most cases correspond to new solution techniques or new simplifications that are tested under the classic mono-period ORPD problem. The contemporary works that have relevance in the current referencing for the construction of a solution to a MP-ORPD problem are presented below.

In [27], a dynamic optimal reactive power flow is carried out taking into account voltage stability. In this case, the problem is solved by means of a branch and bound primal-dual interior point method and different areas are considered. The amount of dynamic reactive power reserves is used as a measure of voltage stability in each area of power system. In this work, the solutions were compared when using discrete variables vs continuous variables, and it is shown that the result of continuous optimization makes the discrete control devices adjust continuously, which is inconsistent with the real situation of the power systems. The proposed model was applied to IEEE 30 and 118-bus test systems and the computational times were 177.94s and 12603.44s, respectively.

In [28], a three-stage programming approach is proposed to achieve a fully decentralized solution to the DRPO problem of the multiarea power system. This preserves the control independence and information privacy of the distributed subnetworks. A forward-backward-pass dynamic programming approach is implemented to solve the stepwise fitting problem. This solution method does not require a central coordinator, involves only minor boundary information exchange between the subproblems, and can handle discrete variables. The solution time much higher with respect to the centralized solution method; however, they implemented a parallel implementation which was not fast but turned out to be competitive.

In [29] and [2] a day-ahead reactive power dispatch is presented. In [29] wind plants are considered within a distribution network, the method of solutions is "Pre-Coarse-Fine" based in a genetic algorithm. The simulations were carried out in the IEEE 33-bus distribution test system and the average solution time is 260s. In [2], an ancillary service procurement problem is presented. This as a bi-objective MP-ORPD that seeks to minimize the cost and voltage deviation under wind power generation uncertainties in a pool-based deregulated system. The voltage deviation is evaluated only in the load buses, with respect to 1 p.u value. The problem is solved using a developed Pareto-based multi-objective artificial electric field algorithm (MO-AEFA). This methodology is tested in the IEEE 30-bus and IEEE 118-bus test systems and the average solutions time are 66.86s and 272.8 s, respectively. The capacitors are assumed to be switchable with steps of 1 MVAr, which is not often found in the current operation of power systems. Furthermore, in both cases [29] and [2] transformer tap changers are not considered as a control variables or within the power flow equations.

In [30], a multi-objective ORPD model that provides, in terms of weighting factors, trade-offs between minimal active power losses in transmission systems and minimal number of control adjustments in generator voltages, tap ratios and shunt controls is featured. The problem is implemented in GAMS and is solved by translating the original MINLP problem into an NLP problem; this by using a bipolar sigmoid function for the binary variables. However, the study only considers the static version of the problem (a

single analysis period); The authors caution that the use of the sigmoid approximation in multi-period problems with coupled time constraints has not yet been tested.

In [8], a coordinated voltage control scheme is treated as a MP-ORPD with voltage security constrains. The voltage control strategy is formulated as a MINLP problem and is solved by means of the Generalized Benders decomposition (GBD). The concept of voltage safety refers to satisfying the chargeability margin defined in a previous study. The proposed methodology is examined through case studies conducted on a simple 6-bus, the IEEE 118-bus, and 1180-bus test systems. The authors do not include the transformer taps within the Y-bus matrix for the AC power flow model, this because a multi-period representation makes repeated calculation of the Y-bus matrix be hard.

In [10], a hybrid metaheuristic is used for solving the dynamic optimal reactive power dispatch (DORPD) problem; note that DORPD and MP-ORPD are the same problem. The described hybrid method employs the Message Passing Interface (MPI) based parallel computation and particle swarm optimization (PSO) algorithm are combined to form the parallel particle swarm optimization (PPSO). Their simulations show that a time-coupled formulation reduces the number of maneuvers in the system, this with respect to individual optimizations. Although the authors mention that the parallelization technique improves computational performance, this is only valid when comparing with other non-deterministic algorithms. Finally, the model of the shunt elements does not represent reality, those elements taking such a small step.

In [9], the authors presented a ORPD with time-varying loads where the objective function is to minimize the power losses and the cost of adjusting the control devices. The solution method used is metaheuristic kwon as 'Cataclysmic Genetic Algorithm'. The authors collected five aspects to be introduced into the MP-ORPD model. These factors are related to the investment of control devices and payments to operators related to reactive power control. In the formulation of the problem, a term is introduced to minimize the number of maneuvers on the tap transformer; however, the way in which the term was posed, finds an average value (a more plane value) of the tap position, instead of minimizing the number of maneuvers without restricting the moving range. Finally, the small scale of the test system does not allow to have solid conclusions about the results shown.

Some other researchers presented that the artificial intelligence can deal with the discrete variables and the limitation of the number of actions in reactive power optimization [31–33]. However, the algorithms employed in their research show low efficiency and unstable optimization results.

2.2 Theoretical framework

2.2.1. The Problem of Optimal Reactive Power Dispatch

The control of reactive power must meet their demand and provide voltage support in the electrical network, both in normal operation and in contingencies, maintaining the quality of the service and seeking efficiency criteria in the operation.

The power system operator together with stakeholder agents coordinate the control of voltages in the different areas; thus, reactive power requirements are guaranteed from a global perspective and satisfying the particular needs of each area. Coordination is carried out through maneuvers that keep the voltages within the permitted ranges and close to the assigned reference values. These target stress values are different for each node of the system and in each period; that is, a node will have several reference values during one operation day; differences that are due to the changing behavior of time varying load and the characterization of the operation in the control area.

One task covered by the planning and coordination of the operation is the correct schedule of the reactive power dispatch. The purpose of the reactive power dispatch model is to determine the configuration of the control variables. Usually with the aim of maintaining a safe voltage profile while meeting network constraints. The model takes as control variables the taps of transformers, the set-point of generators, the reactors, and the

capacitors. The input data is the active power dispatch schedule (which ideally should not be altered).

In the optimal dispatch of reactive power, one or more objectives can be set, and the constraints of the problem guarantee the nodal balance, respect the limits and parameters of lines, generators, capacitors, reactors and transformers. In the literature [34–36] the objectives developed with the highest recurrence are of three types:

- Minimization of losses, generally associated with the sum of total active power losses through the connection elements.
- Voltage stability index, which evaluates long-term voltage stability.
- Deviation functions (function: voltage and/or operation of control elements).

Traditionally, the reactive power dispatch problem was solved by the system operators using techniques based on their experience and sensitivity of the analysis network (a method that continues to be applied in several control centers). However, given that in real systems there are a large number of supervised elements, the network is constantly expanding, and operating maneuvers may vary according to the operator's experience, this makes it necessary for the problem to be solved by optimization techniques. The optimization process should ensure that the solution:

- Corresponds to the actual operating conditions of the system.
- Use the experience of the operator and particular conditions of the network.
- Ensure quality of supply and safe operation.
- The computation times are within the range of analysis and operational planning horizon.

In addition to the above, some relevant aspects of the network must be taken into account. For example, equipment that works in a coordinated manner, such as transformers working in parallel and generators in the same plant, dynamic reactive power reserves and hours of greatest need for these reserves; thus, the particularities of the network must be appropriately characterized within the mathematical model. The operation of electrical power systems involves a certain heuristic component, such as the preference in the use of controls or restrictions on the number of operations of a piece of equipment or devices in a period of time. The knowledge of possible operating scenarios (demand, generation, and topology) allows making early decisions coupled with optimization. These issues should be included in the formulation of the ORPD so that its solution is useful for operators.

2.2.1.1 General structure

Most ORPD formulations are usually represented using the following standard form:

$$\begin{aligned} &\min f(u,x) \\ &\text{s.t } g(u,x) = 0 \\ &h(u,x) \leq 0 \end{aligned}$$

The objective function $f(u, x)$ represents the optimization objective of the system. f is a scalar function, but in multi-objective ORPD it can be interpreted as a vector function. The vector functions $g(u,x)$ and $h(u,x)$ represent equality and inequality constraints respectively. Depending on the selection of f, g and h, the ORPD can be a non-convex and nonlinear problem, a nonlinear problem or a nonlinear mixed integer problem.

In general, the computational challenge of solving an ORPD formulation increases substantially with the accuracy of the system representation. The presence of non-convexity in the targets and constraints make ORPD problems especially challenging, both computationally and theoretically [37]. Furthermore, structurally "complicated" constraints are difficult to handle in random or stochastic search techniques.

2.2.1.2 Variables

Control variables generally represent the configuration of the control device; These can be continuous or discrete and differ widely between ORPD formulations depending on the nature of the particular problem being considered. Table 1 summarizes the variables found in the literature together with representative references.

Table 1. ORPD problem variables

Variable	Type	Reference
Regulated bus voltage magnitude	Continuous	[13]
Transformer tap settings	Continuous, Discrete	[38]
Switched shunt reactive devices	Discrete	[30]
Real/reactive power generation	Continuous	[13]
FACTS controls	Discrete, Continuous	[3]
HVDC link MW controls	Continuous	[39]

2.2.1.3 Objetives

The ORPD can be formulated as a problem with one or more objectives whose purpose is to determine the optimal configuration of the decision variables. System Operators generally seek to meet a grouped set of requirements for the power system, which in the optimization problem conflict, that is, the improvement of one objective occurs at the expense of the other objectives of the group. The way in which single-objective and multi-objective problems are solved are different, since the solution of a multi-objective problem does not have a single representation; instead, a cloud of solutions, representing trade-offs of the different objectives is given. However, multi-objective optimization problems can be formulated into a single-objective problem by introducing weighting factors that transform the objectives into a single weighted objective. Table 2 summarizes the objective functions found in the literature together with representative references.

Table 2. ORPD problem objectives

Objetive	Reference
Active/reactive power loss	[15]
Voltage stability index	[20,40]
Number of controls	[30]
Optimal voltage profile	[13,20]
Total reactive power cost	[2]
Reactive power reserve	[41]
Loading margin	[41]
Operation & maintenance cost of wind farm	[15]

2.2.1.4 Constraints

The ORPD constraints can be classified into equality constraints and inequality constraints, summarized in Table 3. The equality constraints $g(u,x)$ include the power flow equations and any other equilibrium constraints. In the literature there are three standard models for AC power flow equations (standard line power): "polar power-voltage", "rectangular power-voltage" and "rectangular current-voltage" and additionally there is an alternate model " Y-bus "; which are both nonlinear and nonconvex.

The inequality constraints $h\ (u,\ x)$ includes minimum and maximum limits on the control and state variables, such as the voltage at the nodes and the magnitudes of the current through the lines. However, other types of restrictions are also modeled within

this set, which can be used to represent stability or the number of control actions, among others.

Table 3. ORPD problem constraints

Constraints	Reference
Full AC power flow	[12]
Active/reactive power generation limits	[40]
Demand constraints	[30]
Bus voltage limit	[13]
Branch flow limits	[13]

2.2.2 Pilot nodes

Real power systems are required to keep an appropriate voltage profile throughout the transmission network in face of the hourly evolution of the load and topological changes. In real-life applications a direct voltage optimization of every bus within the entire power system is impractical [42]. Satisfying the objective in a larger node system takes more time and it is not possible when the tolerance margins in each are not well defined, while a representative set is more manageable. A pilot node can be defined as one that represents a set of nodes and their behavior in terms of voltage sensitivity against reactive power sources [11]. A characteristic of a pilot node is its poor relationship with other pilot nodes, so that independence between voltage control areas can be approximated. To find pilot nodes, different authors have developed techniques based on: optimization, statistics, metaheuristics, empirical, unsupervised classification, combinatorial problems, among others [43]. A detailed description of these methodologies is out of the scope of the present work. Therefore, the pilot nodes reported in [11] are used, which presents the identification of voltage control areas based on voltage stability for some IEEE test system.

2.2.3 About the solution methods

The ORPD solution has three ways to be approached, this is through deterministic, non-deterministic and hybrid methods (which are usually categorized within the set of non-deterministic methods). Each of these three categories is extensive and contains a subset of major methods, which in turn result in variations and improvements on the original methods. Research in solving techniques for optimization problems is a field that is in continuous development.

Given the non-linear and non-convex nature of the ORPD problem a bunch of techniques have also been proposed for its solution; a detailed classification of metaheuristic and comparison can be consulted in [36]. However, all the metaheuristics discussed tend to be computationally intensive. As a result, the scalability of non-deterministic OPF methods often lags that of well-developed deterministic OPF methods, even for MINLP formulations [44]. For example, Biskas et al. [45] showed that dynamic PSO and enhanced GA were slower and achieved inferior solutions than using relaxation methods to solve MINLP OPF formulations using commercially available NLP solvers. Some methods are more sensitive to the parameter and penalty choices than others, affecting their computation time as well as theoretical convergence properties. This makes comparisons between methods difficult, as poor parameter selection may make a certain method appear artificially slow in comparison to its peers [22]. A detailed description of the techniques applied to the ORPD problem is outside the scope of this document.

Chapter 3

Proposed mathematical modeling

To solve an optimal reactive power flow problem, it is necessary to formulate an AC power flow model, since the characteristics of the DC power flow approaches do not allow control over the variables related to voltage and reactive power. Within the AC power flow model, power transmitted through lines may experience loss, and this is reflected in the calculations of active and reactive power. Regarding power balance constraints there are several formulations for AC power flow equations, the most popular are three:

- Polar power-voltage (P) uses the polar form of complex quantities and explicitly uses sines and cosines in the power flow constraints.
- Rectangular power-voltage (R) uses the rectangular form of complex quantities, resulting in quadratic power flow constraints with respect to these quantities. Unlike the polar formulation, the sines and cosines are of constant parameters and the bus voltage is separated into real and imaginary parts.
- Rectangular current-voltage (IV) considers the flow of current instead of power on a line. Therefore, the model computes real and reactive current on a line, instead of the real and reactive power on a line. Like the rectangular power-voltage model, the IV formulation uses the rectangular form of complex quantities. Therefore, the line flow constraints are once again quadratic in nature with constant sine and cosine quantities.

Each formulation has two versions to construct the problem, one uses the admittance matrix, which is known as Y-bus and the other one uses a summation of transmission line power flows to calculate power balance equations at every node. While the Y-bus matrix formulation benefits from eliminating the line flow parameters in the bus balance constraints, the benefit is lost when the line flow variables still need to be defined to maintain the line flow limits. For this reason, Standard Line Power (SLP) models (P, R, IV) typically outperform Y-bus models due to the additional calculation required. A detail description of these models can be consulted in [46].

The model of the AC power flow equations presented in the thesis is taken from the work of Lisa Tang and Michael Ferris of the University of Wisconsin (2015) [46]. They conclude that “Polar power-voltage formulation with the SLP version shows the *best performance in terms of the convergent speed*, and rectangular current-voltage formulation tends to find a different local solution for some cases but converges to an optimal solution slightly slower than the polar power-voltage formulation”. In addition, the University of Wisconsin elaborated a comparison of the results of the objective function of the AC polar optimal flow model vs. Matpower, where in both cases the same objective value is reached for the IEEE 57 and IEEE 118 systems. This information on the comparison is available in the "neos-server" web page in the "opf-matpower-comparison" section [53]. The above allows us to validate the model proposed in this thesis, since it uses the same equations as the AC polar power flow model.

The proposed MP-ORPD is subject to equality and inequality constraints [3]. The former consider the definition of power flows as well as the power balance equations derived

from the Kirchhoff's laws, while the latter impose physical limits of variables, and includes additional considerations regarding the maneuvering of equipment (inequality constraints). In this case, the maneuvers of equipment are limited in each period, and a maximum daily limit of movements is also considered.

3.1 Nomenclature

The nomenclature used through the document is provided here for quick references:

3.1.1 Sets

$\mathcal{N}$	Set of buses in the transmission network
$\mathcal{G}$	Set of generators in the transmission network
$\mathcal{C}$	Set of connections in the transmission network
$\mathcal{H}$	Set of interfaces
$\mathcal{T}$	Set of periods
$\mathcal{L}$	Set of branches in the transmission network
$\mathcal{T} \subseteq \mathcal{L}$	Set of transformers with tap charge $\mathcal{T}$ belonging to set of branches $\mathcal{L}$
$\mathcal{S}$	Set of maneuverable shunt elements
$\mathcal{E}$	Set of non-maneuverable shunt elements
$\mathcal{G}_i \in \mathcal{G}$	Subset of generators $\mathcal{G}$ connected to bus $i \in \mathcal{N}$
$\mathcal{G}_{slack} \in \mathcal{G}$	Subset of generators $\mathcal{G}$ connected to slack bus $slack \in \mathcal{N}$
$\mathcal{S}_i \in \mathcal{S}$	Subset of maneuverable shunt elements $\mathcal{S}$ connected to bus $i \in \mathcal{N}$
$\mathcal{L}_l \subseteq \mathcal{L}$	Subset of lines $\mathcal{L}$ belonging to interface $l \in \mathcal{H}$
$\mathcal{N}_\mathcal{P} \subseteq \mathcal{N}$	Subset of nodes $\mathcal{N}$ belonging to pilot nodes $\mathcal{P} \in \mathcal{N}$

3.1.2 Parameters

$G^{\mathcal{L}}_{ijc}, B^{\mathcal{L}}_{ijc}$	Conductance and susceptance on line $ijc \in \mathcal{L}$
$G^{\mathcal{E}}_{i}, B^{\mathcal{E}}_{i}$	Shunt conductance and susceptance at bus $i \in \mathcal{N}$
$B^{\mathcal{C}}_{ijc}, \phi_{ijc}$	Branch charging susceptance and angle on line $ijc \in \mathcal{L}$
$V_{ref,it}$	Reference voltage at bus $i \in \mathcal{N}_\mathcal{P}$ for period t
$B^{\mathcal{S}}_{k}$	Shunt susceptance of shunt element $k \in \mathcal{S}$
$N^{\mathcal{S}}_{k}$	Maximum number of steps of element $k \in \mathcal{S}$
D^{P}_{it}, D^{Q}_{it}	Real and reactive power demand at bus i for period t
$\underline{P_g}, \overline{P_g}$	Lower and upper active power injection limits of generator $g \in \mathcal{G}$
$\underline{Q_g}, \overline{Q_g}$	Lower and upper reactive power injection limits of generator $g \in \mathcal{G}$
$\underline{V_i}, \overline{V_i}$	Voltage magnitude lower and upper limits at bus $i \in \mathcal{N}$
$\underline{\alpha_{ijc}}, \overline{\alpha_{ijc}}$	Lower and upper limit tap position of transformer $ijc \in \mathcal{T}$
$\overline{F^{P}_{ijc}}$	Real power limit on line $ijc \in \mathcal{L}$
$\overline{F^{\mathcal{H}}_{l}}$	Real power limit on interface $l \in \mathcal{H}$
U_{gt}	Status of generator $i \in \mathcal{G}$ in period t
$\overline{M}$	Maximum number of maneuvers allowed in set of periods
$\beta_1, \beta_2, \beta_3$	Penalty factors associated to objective function

3.1.3 Variables

$u^{\mathcal{T}}_{ijct}$	Maneuver on tap transformer $ijc \in \mathcal{T}$ in period t (1: Control action performed)
$u^{\mathcal{S}}_{kt}$	Maneuver on shunt element $k \in \mathcal{S}$ in period t (1: Control action performed)

v_{it}	Voltage at bus $i \in \mathcal{N}$ in period t
θ_{it}	Angle at bus i: $(ijc) \in \mathcal{L}$ in period t
α_{ijct}	Ratio of tap transformer $ijc \in \mathcal{T}$ in period t
$n_{kt}^{\mathcal{S}}$	Step number of shunt element $k \in \mathcal{S}$ in period t
$f_{ijct}^{P}, f_{ijct}^{Q}$	Active and reactive power flowing on line $ijc \in \mathcal{L}$ in period t
$p_{gt}^{\mathcal{G}}, q_{gt}^{\mathcal{G}}$	Active and reactive power generated by generator g in period t

3.2 Objective function

In section 2.2.1.3 of the theoretical framework, the set of objective functions typically used in the reactive power optimization problem is presented. These are adapted according to the needs or particularities of the power system and to the decisions made by operating engineers (who are delegated the task of coordinating the maneuvers for voltage control). The proposed objective function (OF), given by equation (1) is made up of three elements described in equations (2), (3) and (4); the intention of each term is that the actions taken are aligned with the decisions made in a real operation control room and each term minimizes the deviations of the control variables period to period. The first term labeled as TVD (Total Voltage Deviation) complies with the voltage reference of the pilot nodes, where the target value is usually the historical average for each hour and day, which reflects the safe condition in which the power system has already operated and it is therefore the desired value. The second term labeled as TQS (Total Reactive Shunt Deviation), seeks to reduce the maneuvers of shunt elements between continuous periods, the purpose of which is to enable the power system operator to carry out voltage control with as few and non-trivial operations as possible. Finally, the third term, labeled as TQG (Total Reactive Generators Deviation), aims at keeping reactive power reserves, that is, the generation units are at a floating point of reactive power to be able to act (quickly) in the event of a system contingency. Thus, although in different works loss minimization is addressed as a test objective function, we have decided not to include it to give relevance to the actions that are usually taken within the real operation of the power system. In this case, β_1, β_2 and β_3 are penalty factors associated with each objective; v_{it} is the voltage magnitude at pilot bus *i* at time *t*; $V_{ref,it}$ is the reference magnitude of pilot bus *i* at time *t*; $n_{kt}^{\mathcal{S}}$ and $n_{k(t-1)}^{\mathcal{S}}$ are the step number of shunt element $k \in \mathcal{S}$ in period t and period $t-1$; $q_{gt}^{\mathcal{G}}$ is the reactive power generated by generator g in period t; finally, $\mathcal{T}, \mathcal{S}$ and $\mathcal{N}p$ are the sets of periods, shunt elements and pilot nodes, respectively.

$$\text{Min } (\beta_1 \text{TVD} + \beta_2 \text{TQD} + \beta_3 \text{TQG}) \tag{1}$$

$$\text{TVD} = \sum_{t \in \mathcal{T}} \sum_{i \in \mathcal{N}_p} \left(v_{it} - V_{ref,it}\right)^2 \tag{2}$$

$$\text{TQD} = \sum_{t \in \mathcal{T}} \sum_{k \in \mathcal{S}} \left(n_{kt}^{\mathcal{S}} - n_{k(t-1)}^{\mathcal{S}}\right)^2 \tag{3}$$

$$\text{TQG} = \sum_{t \in \mathcal{T}} \sum_{g \in \mathcal{G}} (q_{gt}^{\mathcal{G}})^2 \tag{4}$$

3.3 Equality constraints

In the proposed MP-ORPD model a set of equality constraints are taken into account regarding power flows in branches and power balance constraints in buses. Equations (5) and (6) define power flow in branches. In this case, f_{ijct}^{P} and f_{jict}^{P} represent the active power flow from bus *i* to bus *j* and vice versa; while f_{ijct}^{Q} and f_{jict}^{Q} in equations (7) and (8), represent the reactive power flows from bus *i* to bus *j* and vice versa, respectively.

Note that the power flow equations are different at each end of the line; this is because the tap ratio transformer α_{ijct} is taken account. $G^{\mathcal{L}}_{ijc}, B^{\mathcal{L}}_{ijc}, B^{\mathcal{C}}_{ijc}$ and ϕ_{ijc} are conductance, susceptance, branch charging susceptance and the angle on line $ijc \in \mathcal{L}$, respectively.

Equations (9) and (10) represent, respectively, the active and reactive power balance constraints derived from the Kirchhoff's laws. Where $P^{\mathcal{G}}_{gt}$ and $p^{\mathcal{G}}_{gt}$ are respectively, the fixed and variable active power of generator g at time t; D^{P}_{it} and D^{Q}_{it} are respectively, the active and reactive power demand at bus i for period t; $G^{\mathcal{E}}_{i}$ and $B^{\mathcal{E}}_{i}$ are the shunt conductance and susceptance at bus $i \in \mathcal{N}$, respectively; finally, $B^{\mathcal{S}}_{k}$ is the shunt susceptance of the shunt element $k \in \mathcal{S}$.

$$f^{P}_{ijct} = \frac{1}{\alpha^{2}_{ijct}} G^{\mathcal{L}}_{ijc} v^{2}_{it} - \frac{1}{\alpha_{ijct}} v_{it} v_{jt} \left(G^{\mathcal{L}}_{ijc} \cos\left(\theta_{it} - \theta_{jt} - \phi_{ijc}\right) + B^{\mathcal{L}}_{ijc} \sin\left(\theta_{it} - \theta_{jt} - \phi_{ijc}\right)\right) \quad ,\forall ijc \in \mathcal{L}; t \in \mathcal{T} \quad (5)$$

$$f^{P}_{jict} = G^{\mathcal{L}}_{ijc} v^{2}_{jt} - \frac{1}{\alpha_{ijct}} v_{it} v_{jt} \left(G^{\mathcal{L}}_{ijc} \cos\left(\theta_{jt} - \theta_{it} + \phi_{ijc}\right) + B^{\mathcal{L}}_{ijc} \sin\left(\theta_{jt} - \theta_{it} + \phi_{ijc}\right)\right) \quad ,\forall ijc \in \mathcal{L}; t \in \mathcal{T} \quad (6)$$

$$f^{Q}_{ijct} = -\frac{1}{\alpha^{2}_{ijct}} \left(B^{\mathcal{L}}_{ijc} + \frac{B^{\mathcal{C}}_{ijc}}{2} \right) v^{2}_{it} - \frac{1}{\alpha_{ijct}} v_{it} v_{jt} \left(G^{\mathcal{L}}_{ijc} \cos\left(\theta_{it} - \theta_{jt} - \phi_{ijc}\right) - B^{\mathcal{L}}_{ijc} \sin\left(\theta_{it} - \theta_{jt} - \phi_{ijc}\right)\right) \quad ,\forall ijc \in \mathcal{L}; t \in \mathcal{T} \quad (7)$$

$$f^{Q}_{jict} = -\left(B^{\mathcal{L}}_{ijc} + \frac{B^{\mathcal{C}}_{ijc}}{2} \right) v^{2}_{jt} - \frac{1}{\alpha_{ijct}} v_{it} v_{jt} \left(G^{\mathcal{L}}_{ijc} \cos\left(\theta_{jt} - \theta_{it} + \phi_{ijc}\right) - B^{\mathcal{L}}_{ijc} \sin\left(\theta_{jt} - \theta_{it} + \phi_{ijc}\right)\right) \quad ,\forall ijc \in \mathcal{L}; t \in \mathcal{T} \quad (8)$$

$$\sum_{g \in \mathcal{G}_{i(i \neq slack)}} P^{\mathcal{G}}_{gt} + \sum_{g \in \mathcal{G}_{slack}} p^{\mathcal{G}}_{gt} - \sum_{(jc):ijc \in \mathcal{L}} f^{P}_{ijct} - \sum_{(jc):jic \in \mathcal{L}} f^{P}_{jict} - D^{P}_{it} - {v_{it}}^{2} G^{\mathcal{E}}_{i} = 0 \quad ,\forall i \in \mathcal{N}; t \in \mathcal{T} \quad (9)$$

$$\sum_{g \in \mathcal{G}_{i}} q^{\mathcal{G}}_{gt} + {v_{it}}^{2} \sum_{k \in \mathcal{S}_{i}} B^{\mathcal{S}}_{k} n^{\mathcal{S}}_{kt} - \sum_{(jc):ijc \in \mathcal{L}} f^{Q}_{ijct} - \sum_{(jc):jic \in \mathcal{L}} f^{Q}_{jict} - D^{Q}_{it} + {v_{it}}^{2} B^{\mathcal{E}}_{i} = 0 \quad ,\forall i \in \mathcal{N}; t \in \mathcal{T} \quad (10)$$

3.4 Inequality constraints

3.4.1 Generators constraints

Equation (11) corresponds to the reactive power limits ($\overline{Q_g}$ maximum and $\underline{Q_g}$ minimum) on the set of generators and FACTS (flexible AC transmission systems) devices on-line. In this case, U_{gt} represents the state of generator g, where 1 indicates on line and 0 otherwise. Equation (12) corresponds to the active power limit ($\overline{P_g}$ maximum and $\underline{P_g}$ minimum), on the set of slack generators on-line (which guarantee the active power balance). The rest of the generators are considered as fixed sources of active power.

$$U_{gt}\underline{Q_g} \leq q^{\mathcal{G}}_{gt} \leq U_{gt}\overline{Q_g} \quad ,\forall g \in \mathcal{G}; t \in \mathcal{T} \quad (11)$$

$$U_{gt}\underline{P_g} \leq p^{\mathcal{G}}_{gt} \leq U_{gt}\overline{P_g} \quad ,\forall g \in \mathcal{G}_{slack}; t \in \mathcal{T} \quad (12)$$

3.4.2. Voltage angle constraints

Equation (13) represents is the angular difference between two connected nodes. This constraint guarantees the stable-state limits for a line power transfer. In the case, the angle values are set lower than the theoretical reference of π / 2.

$$-\frac{\pi}{3} \leq \theta_{it} - \theta_{jt} \leq \frac{\pi}{3} \quad ,\forall (ij): ijc \in \mathcal{L};\ t \in \mathcal{T} \quad (13)$$

3.4.3. Transformer constraints

Equation (14) indicates the maximum ($\overline{\alpha_{ijc}}$) and minimum ($\underline{\alpha_{ijc}}$) limits of the ratio transformer (α_{ijct}). Equation (15) is activated when the tap transformer is operating ($u^{\urcorner}_{ijct}$, 1: represent a maneuver, 0 otherwise).

$$\underline{\alpha_{ijc}} \leq \alpha_{ijct} \leq \overline{\alpha_{ijc}} \quad ,\forall ijc \in \urcorner; t \in \mathcal{T} \tag{14}$$

$$|\alpha_{ijct} - \alpha_{ijc(t-1)}| \leq u^{\urcorner}_{ijct} \quad ,\forall ijc \in \urcorner; t \in \mathcal{T} \tag{15}$$

3.4.4. Shunt constraints

Equation (16) sets limits for the number of steps in shunt elements, where $n^{\mathcal{S}}_{kt}$ is the step number of shunt element $k \in \mathcal{S}$ in period t and $N^{\mathcal{S}}_{k}$ is the maximum number of steps of element $k \in \mathcal{S}$. Equation (17) is activated when the number of steps from one period to another one changes, it indicates an action control on the shunt element ($u^{\mathcal{S}}_{kt}$, 1: represent a maneuver, 0 otherwise).

$$0 \leq n^{\mathcal{S}}_{kt} \leq N^{\mathcal{S}}_{k} \quad ,\forall\ k \in \mathcal{S}; t \in \mathcal{T} \tag{16}$$

$$|n^{\mathcal{S}}_{kt} - n^{\mathcal{S}}_{k(t-1)}| \leq u^{\mathcal{S}}_{kt} N^{\mathcal{S}}_{k} \quad ,\forall\ k \in \mathcal{S}; t \in \mathcal{T} \tag{17}$$

3.3.5. Security constraints

Equation (18) determines the limits of voltage magnitude v_{it} for each bus at every time interval t ($\overline{V_i}$ maximum and $\underline{V_i}$ minimum). Equation (19) defines the active power limit ($\overline{F^{\mathcal{H}}_{l}}$) for interface l. Equation (20) indicates the maximum value of active power allowed by each transmission line ($\overline{F^{P}_{ijc}}$).

$$\underline{V_i} \leq v_{it} \leq \overline{V_i} \quad ,\forall\ i \in \mathcal{N}; t \in \mathcal{T} \tag{18}$$

$$\sum_{ijc,jic \in \mathcal{L}_l} f^{P}_{ijct} \leq \overline{F^{\mathcal{H}}_{l}} \quad ,\forall\ l \in \mathcal{H}; t \in \mathcal{T} \tag{19}$$

$$-\overline{F^{P}_{ijc}} \leq f^{P}_{ijct} \leq \overline{F^{P}_{ijc}} \quad ,t \in \mathcal{T}; ijc \in \mathcal{L} \tag{20}$$

3.3.6. Operating times constraints

Equation (21) indicates that the total number of maneuvers on capacitors, reactors and transformer taps must not exceed the maximum set in one day of operation. In this case, $u^{\urcorner}_{ijct}$ is the maneuver on tap transformer $ijc \in \urcorner$ in period t, $u^{\mathcal{S}}_{kt}$, is the maneuver on shunt element $k \in \mathcal{S}$ in period t, and $\overline{M}$ indicates the maximum number of maneuvers allowed.

$$\sum_{t \in \mathcal{T}} \left(\sum_{ijc \in \urcorner} u^{\urcorner}_{ijct} + \sum_{k \in \mathcal{S}} u^{\mathcal{S}}_{kt} \right) \leq \overline{M} \quad ,\forall\ t \in \mathcal{T}; k \in \mathcal{S};\ ijc \in \urcorner \tag{21}$$

The MP-ORPD model presented in this document is a non-linear, non-convex optimization problem classified as a mixed-integer nonlinear programming (MINLP) problem as it handles continuous, integer, and discrete control variables. A MINLP problem is said to be convex if its continuous relaxation, i.e. the problem obtained by dropping the integrality constraints, is a convex optimization problem; otherwise, it is said to be nonconvex. Note that in this case, equality constraints include the multiplication of variables as well as sine and cosine functions of voltage angles. Also, absolute values are included in equations (15) and (17).

Chapter 4

Tests and Results

4.1 Description of the test systems

Several simulations were performed on the IEEE 57-bus and 118-bus test systems (original models without FACTS devices). The data for these systems can be consulted in [48]. All tests were carried out on a personal computer equipped with an Intel Core i5 (Quadcore) 1.8 GHz processor and 8 GB of RAM memory. The proposed MP-ORPD model was implemented in General Algebraic Modeling System (GAMS, version 24.8.5), using BONMIN solver [49]; the algorithm used in our case was BONMIN-DiveMIPFractional. The algorithms in BONMIN are exact and ensures global optimal when both the objective function and constraints are convex, otherwise they are heuristics [49,50] which is the case in the ORPD problem. Since BONMIN uses branch-and-bound based algorithms which utilize NLPs for bounding, it often finds good solutions (but not necessarily global) also for nonconvex problems [49]. This is in contrast with pure outer approximation-based algorithms which may easily run into infeasible linear or mix integer programming relaxations due to wrong cutting-planes [50].

The MP-ORPD contemplates time-varying loads. In this document, load conditions are featured through a load curve of a spring weekday available in [51]. The behavior of the 24-h load curve for both test systems is illustrated in Figure 1, where each of the four colors, represents a load condition with which the reference voltage value was chosen for the pilot nodes; these are: purple (minimum-load), blue (medium-load), orange (high-load) and gray (low-load). Figure 1 illustrates the time varying load of the IEEE 118-bus test system. A scale factor of 0.2947 is used to obtain the load of the IEEE 57-bus test system.

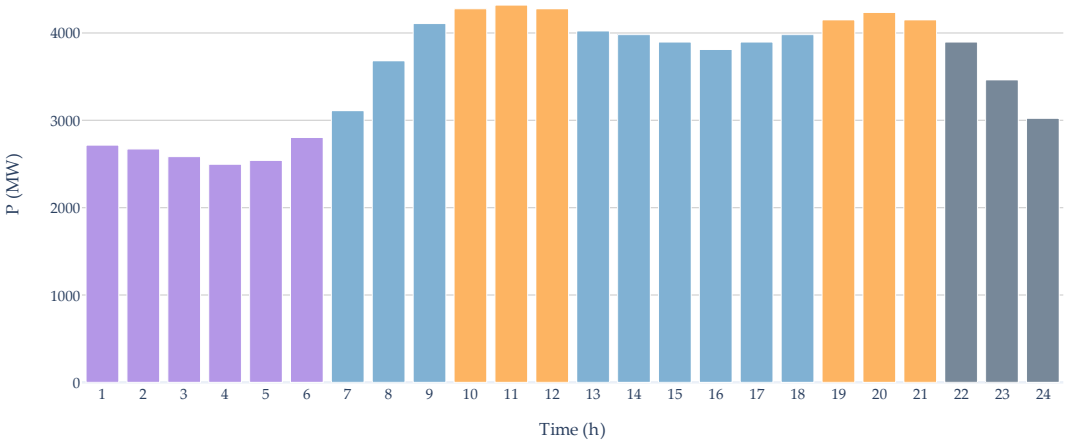

Figure 1. 24-h load curve performed of IEEE 118-bus test system

4.1.1 IEEE 57-bus test system

The IEEE 57-bus test system consists of 62 branches and 26 control variables; these include 7 generation units, 16 transformers and 3 capacitors. The single-line diagram of the system is depicted in Figure 2, where each color represents a different voltage control area with a single pilot node. The total active and reactive load demand is 1250 MW and 336 MVAr for period 11 on 100 MVA base. The initial output of active and reactive power of generators comes from the solution of the Unit Commitment (UC) problem reported in [46]. Also, the initial settings of the tap transformers are in the nominal ratio and all shunt elements are connected.

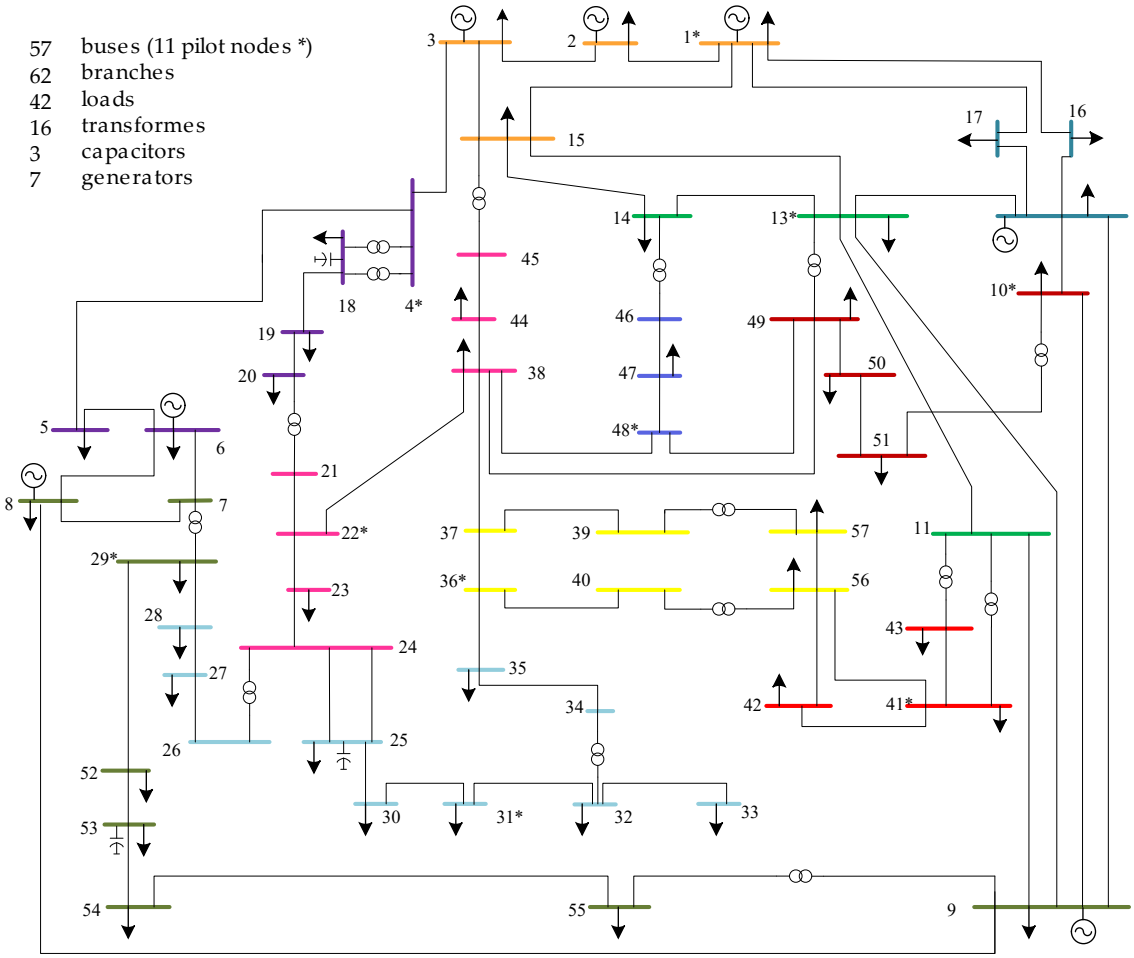

Figure 2. IEEE-57 Single-line diagram, annotated with pilot nodes and voltage control areas

Minimum and maximum limits of control variables for the IEEE 57-bus test system are as follow: each transformer ratio varies from 0.9 to 1.1 per-unit (p.u) in equal steps of 0.01. Shunt elements are between 0 and its MVAr parameter, these have no steps. Voltage set-points of generators vary in the range [0.85, 1.1] p.u (except for lower voltage limit of the pilot nodes, which are reported in Table 4). Table 4 shows the shunt MVAr parameter as well as lower voltage limits for pilot nodes taken from [11]. In this case, the maximum number of maneuvers allowed in a day ($\overline{M}$) is set to 150.

Table 4. Lower voltage limits of pilot nodes and MVAr parameter of shunt elements (IEEE 57-bus test system).

Pilot Node	Lower voltage limit (p.u)	Shunt	MVAr
V_{np1}	0.9097	Q_{C18}	10
V_{np4}	0.9177	Q_{C25}	25
V_{np10}	0.9244	Q_{C53}	53
V_{np12}	0.9252		
V_{np13}	0.9039		
V_{np22}	0.8927		
V_{np29}	0.9274		
V_{np31}	0.8500		
V_{np36}	0.8640		
V_{np41}	0.9119		
V_{np48}	0.9038		

4.1.2 IEEE 118-bus test case

Several simulations were performed on the IEEE 118-bus test system, which has 186 branches and 77 control variables; these consist of 54 generation units, 9 transformers, 12 capacitors and 2 reactors. The single-line diagram of the system is depicted in Figure 3, where each color represents a different voltage control area with a single pilot node. The total active and reactive base loads are 4242 MW and 1438 MVAr for period 11 on 100 MVA base. The initial output of active and reactive power of generators comes from the solution of a UC problem reported in [46]. Also, the initial settings of the tap transformers are in the nominal ratio and the state of shunt elements are all connected.

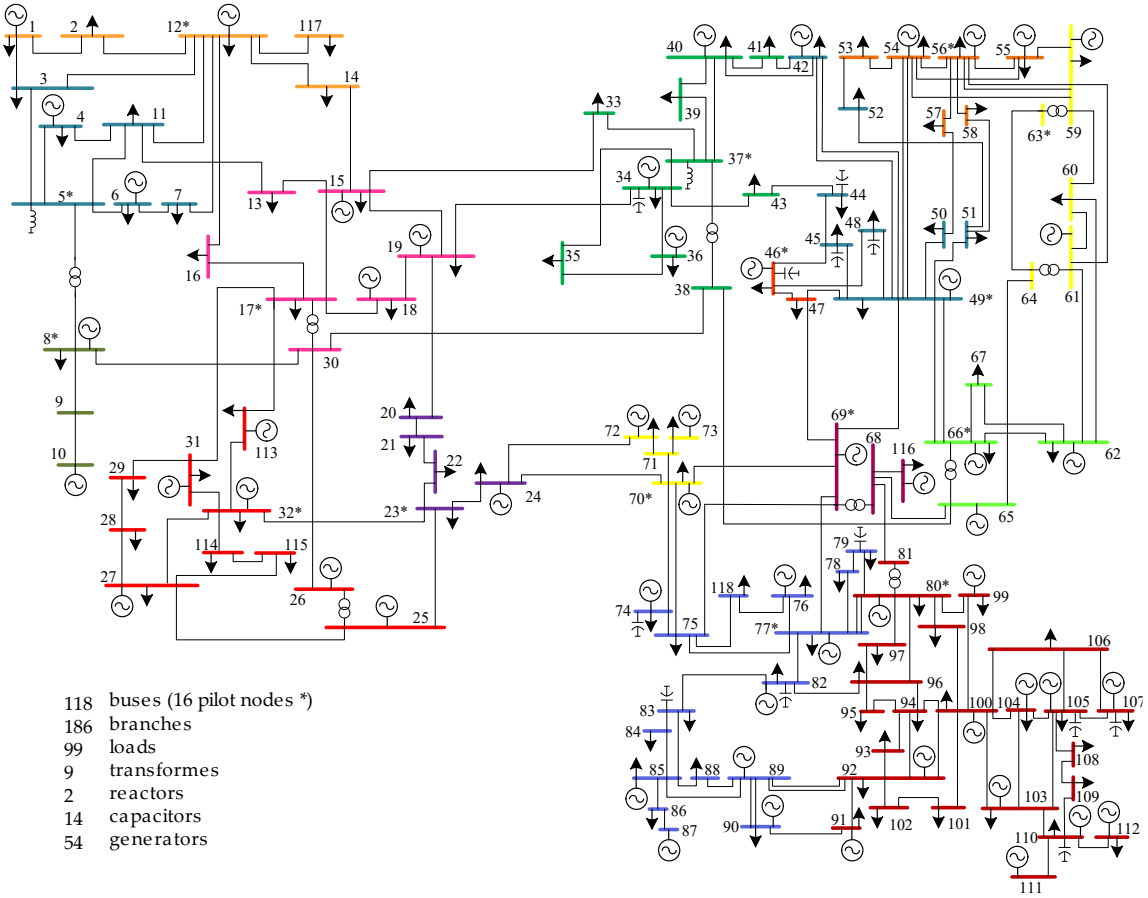

Figure 3. Single-line diagram of the IEEE118-bus test system with pilot nodes and voltage control areas.

Minimum and maximum limits of control variables for the IEEE 118-bus test system are as follow: each transformer ratio varies from 0.9 to 1.1 p.u in equal steps of 0.01. Shunt elements are between 0 and its MVAr parameter, these have no steps. Voltage set-points of generators vary in the interval [0.9, 1.1] p.u (except for lower voltage limits of pilot nodes, these are reported in Table 5). Table 5 shows the shunt MVAr parameter and lower voltage limit for pilot nodes taken from [11]. In this case, $\overline{M}$ is set to 100 in all operation day.

Table 5. Lower voltage limits of pilot nodes and MVAr parameter of shunt elements (IEEE 118-bus test system).

Pilot Node	Lower voltage limit (p.u)	Shunt	MVAr
V_{np69}	0.935	Q_{L5}	-40
V_{np5}	0.9481	Q_{C34}	14
V_{np37}	0.9276	Q_{L37}	-25
V_{np56}	0.9427	Q_{C44}	10
V_{np77}	0.9349	Q_{C45}	10
V_{np66}	0.90	Q_{C46}	10
V_{np46}	0.9341	Q_{C48}	15
V_{np23}	0.90	Q_{C74}	12
V_{np12}	0.932	Q_{C79}	20
V_{np70}	0.9434	Q_{C82}	20
V_{np17}	0.90	Q_{C83}	10
V_{np63}	0.90	Q_{C105}	20
V_{np80}	0.954	Q_{C107}	6
V_{np8}	0.9655	Q_{C110}	6
V_{np49}	0.9542		
V_{np32}	0.90		

4.2 Results

The schedule of control variables for the MP-ORPD (on IEEE 57-bus and 118-bus test systems) is reported in Appendix A, it indicates the settings for capacitors, reactors, transformers and generation voltages period to period. It was possible to verify that all the variables were kept within their operative ranges. All results below subsections correspond to the complete OF (TQG+ TVD+TQD) given by equation (1). In each study case we compared the optimization result vs. a base case. The base case represents the system condition where only the active power dispatch has been optimized; therefore, there are no objectives related to the voltage setpoint, nor to the reactive power management in the compensation elements and generators. The base case is taken as a reference to show the difference between the result of the MP-ORPD optimization and the system input information, which allows to understand how the control variables have changed.

4.2.1. IEEE 57-bus test system

Figure 4 depicts the voltage profile curves of four pilot nodes. Note that the voltage control implemented in this system fits the reference curve proposed for each pilot node. The shape of the voltage profiles of the pilot nodes is in accordance with the operational strategy that increases the reference values of these nodes at peak demand in order to guarantee the voltage stability of the system.

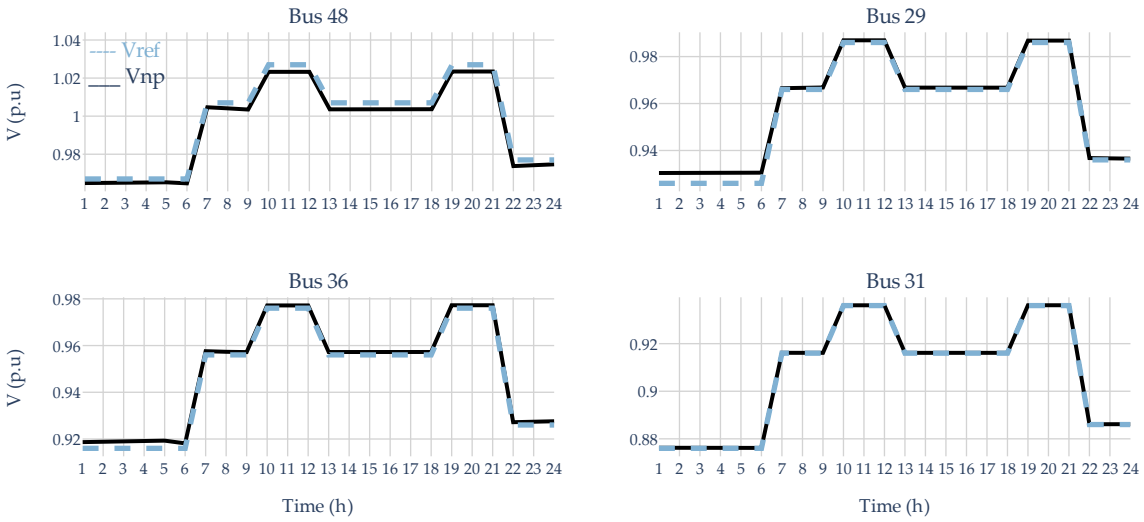

Figure 4. Voltage profiles of pilot nodes (48, 29, 36 and 31) for IEEE 57-bus system.

The proposed system has a high reactive power demand and must meet the voltage profiles required in the pilot nodes as shown in Figure 4. In addition, of the 26 control elements, only 10 have the capacity to provide reactive power and of these, 7 are generation units and 3 capacitors. This evidences that the IEEE 57-bus test system is quite limited for an adequate reactive power dispatch. Figure 5 shows the reactive power output of all generators of the system per period. In periods of low demand, in order to obtain the desired voltage in the pilot nodes, it is necessary to increase the amount of reactive power injected, while for periods of medium and high demand, a smaller increase in reactive power injection is observed. This behavior is an indicator of depletion of reactive power reserves, and provides signals for expansion of reactive power sources. Additionally, from the results of the optimization Table A1 of Appendix A, it is possible to understand that when there are capacitors and reactors with little or no movement, these elements do not contribute to the flexibility of the network, but they solve a specific need. Expansion must be accompanied by flexibility, points with little flexibility tend to have a low-quality voltage regulation; the contingency in any of these compensation elements may result in voltage objectives out of range or greater use is made of the reactive power reserve in the generators.

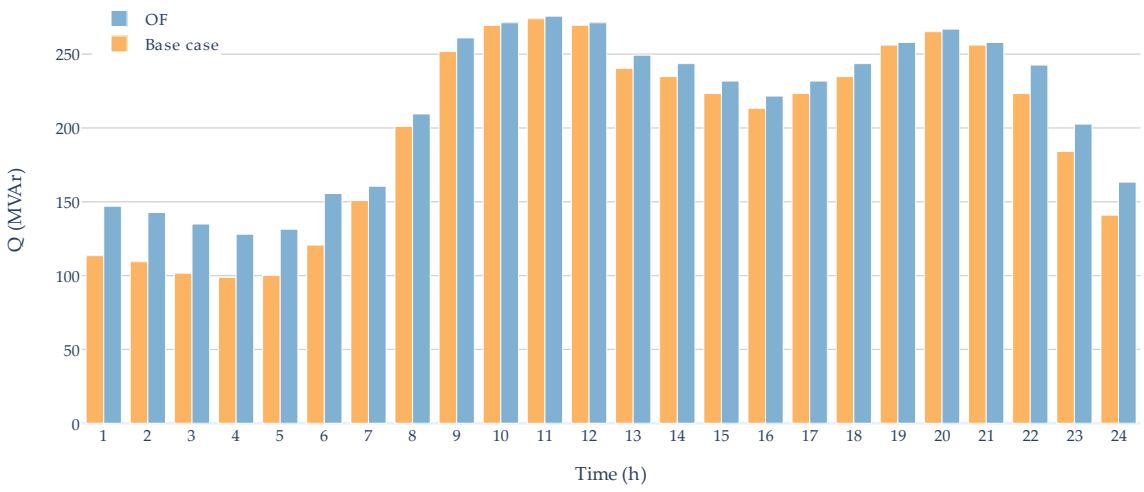

Figure 5. Absolute reactive power output of generators per period for IEEE 57-bus system

Figure 6 shows the operation of the taps for four randomly selected transformers. They behave according to the demand of the control area of each pilot node and the availability of shunt elements and generators. The area controlled by transformer T10-51 has this one as the only control element; therefore, its behavior features a greater number of maneuvers, while transformers T24-26 and T7-29 have internal or nearby control elements such as shunt compensation, generation and the transformers themselves, which is why the number of maneuvers for these elements is lower.

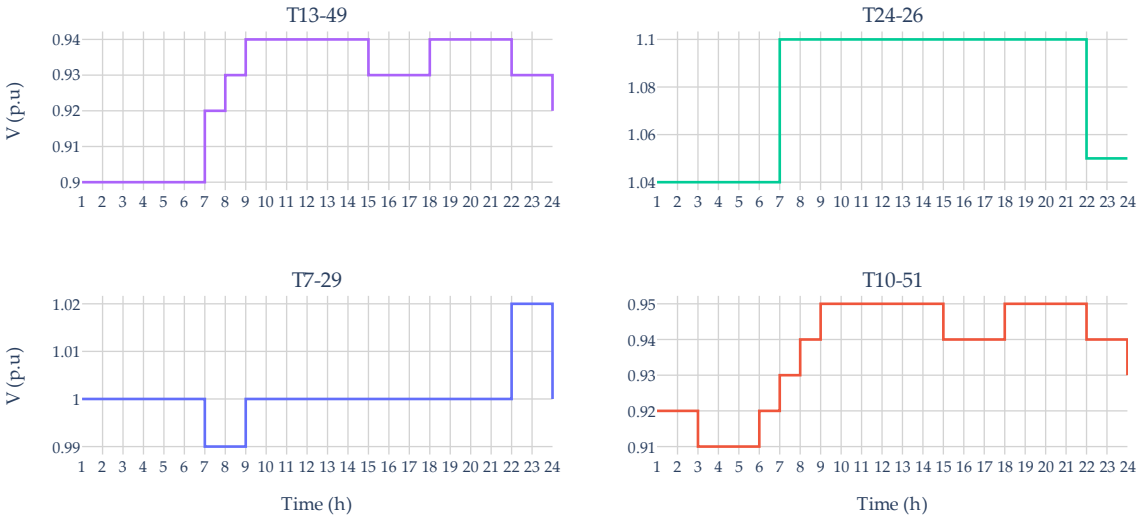

Figure 6. Tap position settings in one operation day (values expressed in p.u) for the IEEE 57-bus test system

4.2.2. IEEE 118-bus test system

One of the objectives within the MP-ORPD is to maintain adequate voltage profiles on the set of pilot nodes. In this document, four settings of voltage values were defined for an operation day: minimum, low, medium and high voltage; which are characterized by the demand behavior and user requirement. Figure 7 shows the reference voltage profiles and the voltage after optimization, this for a sample of pilot nodes (5, 63, 46 and 8). Additionally, as a particular case, bus 5 was set with a higher voltage profile in the peak periods (0.058 p.u, with respect to its minimum reference and a 138 kV voltage base). The results show that even with an "aggressive" voltage profile it is possible to follow the voltage reference value.

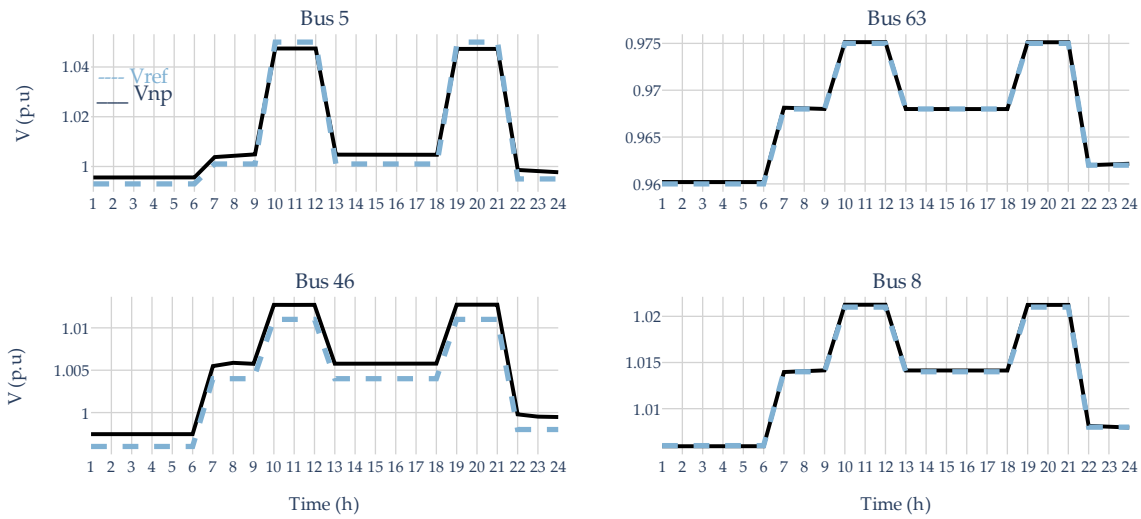

Figure 7. Voltage profiles of pilot nodes (5, 63, 46 and 8) for the IEEE 118-bus test system.

The maximum error between the reference and the optimized voltage is less than 0.95kV as shown in Figure 8, where the indicated period is not the same in each node, but the period with the greatest difference; in Figure 8 the pilot node 49 at period 11 has an error of -0.94 kV, this difference is not constant in the other periods has a lower absolute value.

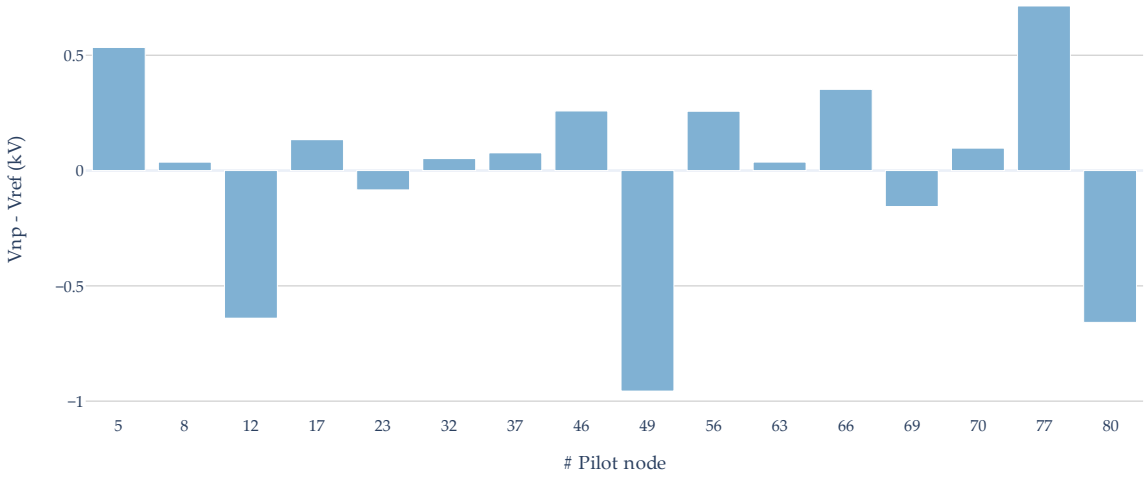

Figure 8. Maximum error between reference and optimized voltage in pilot nodes (kV) for the IEEE 118-bus test system.

The sum of reactive power in absolute value of the set of generators at each period is a way of representing the use of the dynamic reactive power reserve, which in a power system is necessary to manage uncertainty and contingencies [52]. Figure 9 presents the dynamic reserve of reactive power in the base case (orange) and its subsequent optimization (blue). In this case, reactive power reserves after optimization represent only 31.3% of the base case. This is important since it allows the system operator to better react in face of disturbances and uncertainty, also, maintaining sufficient reactive reserves at the most quickly and effectively VAR sources is intrinsic requirement for proper corrective control actions.

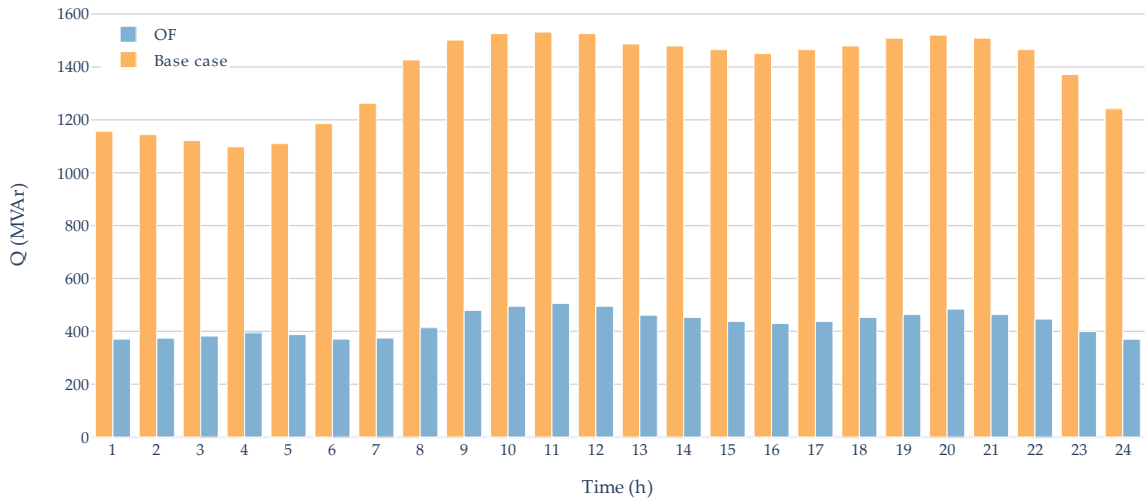

Figure 9. Absolute reactive power output of generators per period for the IEEE 118-bus test system.

In this case, compared to the 57-bus system, there are about three times as many elements to control the reactive dispatch, so the system is able to follow the voltage profile of the pilot nodes.

Figure 10 presents the reactive power output per generator, this for a sample of the set of generators in a random period (in this case: gen 4, 10, 59, 69, 77 and 90; period 11). It is observed a significant reduction in reactive power in the optimized case (blue) vs the base case (orange).

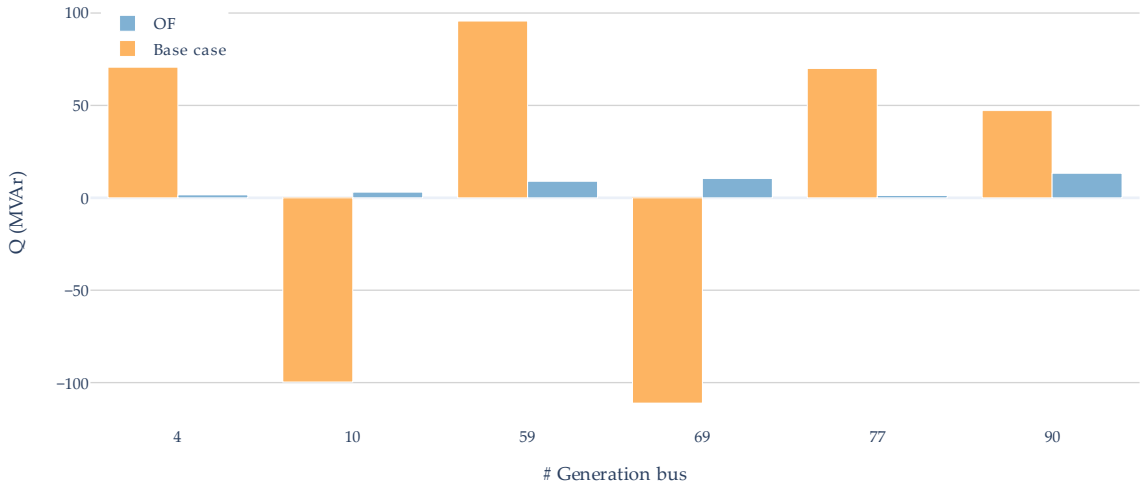

Figure 10. Reactive power output of generators (4, 10, 59, 69, 77 and 90) at period 11 for the IEEE 118-bus test system.

Figure 11 shows the variation of tap positions (expressed in terms of ratio) per transformer throughout a day of operation. It is observed that the number of maneuvers on the tap is greater during periods with high demand and high voltage profiles; nonetheless, the maximum number of maneuvers is kept as indicated in equation (21).

These results evidence the relationship between the number of transformer operations and the availability of additional elements for reactive power control. When in a given area there are other elements for reactive power control, apart from the transformers, the number of maneuvers in these elements is reduced. This is the case of transformers T81-80 and T8-5, which are located in small control areas with other elements that provide reactive power control, resulting in lower transformer maneuvers.

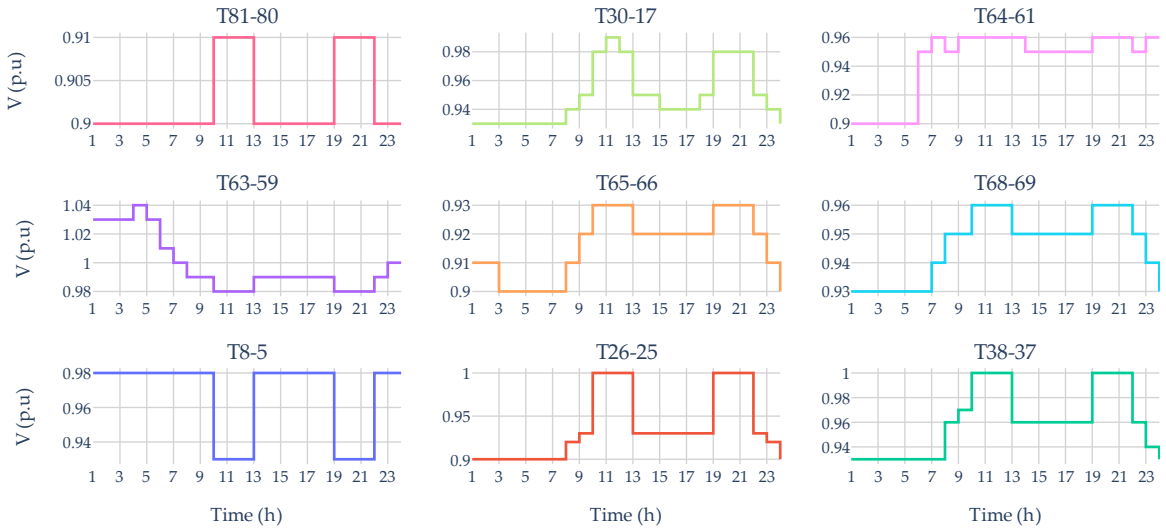

Figure 11. Tap position settings in one operation day (values expressed in p.u) for the IEEE 118-bus test system

4.3 Sensibility of objective function components

Table 6 shows a sensitivity analysis of results for the IEEE 57-bus test system. The first row shows the total number of taps operations. The second row corresponds to the total number of operations on shunt elements; while the third and fourth rows indicate the reactive deviation of the generators and the voltage deviation with respect to the pilot nodes, respectively. When evaluating a single objective, the proposed approach manages to reduce the objective function considerably. For the case of reactive deviation, the formulation that only considers TQG is the lowest of all the cases analyzed, while the lowest number of maneuvers is achieved with the TQD formulation, with a total value of 51 maneuvers; similarly, it is observed that the lowest voltage deviation with a value of 0.18 is obtained with the TVD formulation. It was already mentioned that this test system needs a higher reactive power support. This fact is evidenced when comparing the maximum and minimum values of the reactive power deviations in generators and the voltage deviations of the pilot nodes. The last column in Table 6 (TQG+ TVD+TQD) indicates the best trade-off in the use of elements for reactive power control; these are results shown in the preview figures, Figures 4–6.

Table 6. Sensibility of the objective function components for IEEE 57-bus system

	Case base	**TQG**	**TQD**	**TVD**	**TQG+ TQD**	**TQG+ TVD**	**TVD+ TQD**	**TQG+ TVD+TQD**
$\sum u_{ijt}^{\tau}$	0	117	51	141	118	118	135	118
$\sum u_{it}^{s}$	0	0	0	4	0	1	0	1
$\sqrt{TQG}$	4757	3928	4588	6965	3928	5101	7080	5101
$\sqrt{TVD}$	10.56	29.94	10.97	0.18	29.9	1.69	0.2	1.69

Table 7 presents a comparison of each component of the objective function and its combinations, this in order to evaluate the individual and joint sensitivity on the objective function. The following metrics are evaluated: the number of maneuvers carried out on the transformer taps, the number of maneuvers on the shunt elements, the absolute value of the reactive power used by the generators and the voltage deviation in the pilot nodes with respect to the reference value; all information corresponds to operation day of 24-h.

Table 7. Sensibility of the objective function components for IEEE 118-bus system

	Case base	**TQG**	**TQD**	**TVD**	**TQG+ TQD**	**TQG+ TVD**	**TVD+ TQD**	**TQG+ TVD+TQD**
$\sum u_{ijt}^{\tau}$	0	85	20	51	72	71	54	78
$\sum u_{it}^{s}$	0	13	0	20	14	19	0	17
$\sqrt{TQG}$	33037	4493	35997	36509	4494	10337	37000	10341
$\sqrt{TVD}$	18.22	20.98	7.37	8E-06	20.98	0.66	4E-12	0.66

For this system, there is a large reactive power reserve, which is evident when comparing the maximum and minimum values of the formulations illustrated in Table 7. For this case, the compared values have a greater range of variation with respect to the IEEE 57-bus test system. The last column in Table 7 (TQG+ TVD+TQD) indicates the best trade-off in the use of elements for reactive power control; these are results shown in the preview figures, Figures 7–11. In this case, the simulation time was 100 s. Note that the use of dynamic reactive power reserves was reduced to more than a third of the base case; in addition, the results followed the voltage profiles successfully.

The simulation times obtained with the objective function given by Equation (1) for the IEEE 57-bus and IEEE 118-bus test systems were 17.5s and 100s, respectively. Additionally, an experiment was performed in which the whole set of nodes was included in

the optimization problem. In this case, the objective voltage profiles of the nodes correspond to the values previously defined in each control area and that were represented by the pilot nodes. The computation times in this experiment were 128s and 239s for the IEEE 57-bus and IEEE 118-bus, respectively. This evidenced that selecting a reduced set of nodes (pilot nodes) improves the computational time of the algorithm.

Chapter 5

Conclusions and future work

5.1 General conclusions

The literature reviewed on the ORPD problem shows a trend of research aimed at representing the real characteristics of the operation within the optimization models. Some of the main aspects in the literature review are: the minimization of maneuvers, the improvement of the voltage profile in the electric network, the representation of reactive power costs in systems that remunerate ancillary services, and the scheduling of elements, among others. There is a great variety in the techniques used for solving the ORPD problem, which provides flexibility to the user depending on the requirements of its implementation. However, it should be noted that the computation times of the non-deterministic techniques reported by the authors turn out to be greater than those that occurred when deterministic solution methods are adopted. To deal with this issue, some authors offer proposals based on the parallelization of the solution techniques, which improves computation times, but continue to be behind the deterministic methods already developed that have implemented a handling of the variables of the integer type. On the other hand, there is the fact that the models described do not have sufficient detail, for example, a large part of the studies consulted omit the representation of the transformer taps in the power flow equations, this being a key aspect to model reactive power flows. Some other works handle the shunt elements as an almost continuous variable where the step is too small, therefore, although there is an intention to bring the models closer to reality, the mathematical representation is not suitable.

This thesis presented a novel approach to the MP-ORPD problem. A new formulation considering three operative goals was described and implemented. The first goal under consideration seek to keep adequate voltage profiles in all the power system through a reduced set of buses (pilot nodes), where the values of the voltage set points are adjusted dynamically; changing every period according to load conditions. The second goal avoid excessive maneuvers on shunt devices, since a large number of these lead to lower life expectation of devices and more maintenance under real-life circumstances. The third goal was designed to maintain the dynamic reactive power reserves of the generators, guaranteeing a fast response to control voltages on contingency scenario.

The main feature of the proposed MP-ORPD model lies on its applicability in real power systems, since it does not follow conventional objective functions such as power loss reduction; instead, it guarantees operative feasibility throughout a given time horizon, while minimizing the number of maneuvers on reactive power devices. Several tests carried out on the IEEE 57-bus and 118-bus test system allowed to prove the effectiveness and applicability of the proposed approach. It was found that the method of weights allows adjusting the priority of the objectives, providing flexibility to the needs of each system under analysis. The decision to choose a set of pilot nodes significantly improves the computation times, this with respect to the optimization on all the system nodes. The time taken for the optimization was 17.5s and 100s for IEEE 57-bus and 118-bus test systems, respectively, which allows concluding that the model can be used in coordinated voltage control strategies, at instances of the day-ahead and very short-term operation planning.

Although dynamic reactive power reserves are considered, voltage stability issues are not explicitly integrated in the model.

5.2 Future work

The results of this research contribute to the current state of the art on MP-ORPD models. It is expected in the future to clear up some additional problems found throughout this work, among which the following stand out:

- Implement a multi-area MP-ORPD model.
- Explore the possibility of parallelization for reducing computational time.
- Use specialized dynamic programming algorithms.
- Explore convexification techniques to ensure global solutions.
- Explore and adapt algorithms and/or solution methods to improve model computation times.
- Implement the proposed model in larger systems.
- Use alternatives to deal with integer variables.
- Consider security constrains about N-1contingencies.

Appendix A

MP-ORPD schedule

A.1 Post-processing method in the transformer tap

The post-processing method employed consists of capturing the tap values resulting from the optimization and approximating this to the closest discrete tap value established (21 steps for each transformer). Then the new tap value is loaded to the GAMS model from being a variable to a parameter, then the AC power flow is run and the deviation of the results of the model run is measured. When the deviation is less than 5% (expert criterion) its value is accepted, in case of being higher, a slack is given to the taps to make the optimization again only with this as a variable. Then it is re-evaluated. casein the tested cases in this work the values were always lower than 5% from the first optimization run.

A.2 MP-ORPD schedule and GAMS structure

The solution program was made in GAMS, it is composed of 4 files and it needs as input a UC solved (the IEEE 57 and IEEE 118 cases, with the 24-h demand curve of chapter 4, are available in [48]), the structure of the solution program is shown in Figure 12. The main file is called *master* and coordinates the other 3 files; The *master* contains the AC power flow equations, the constraints, the calculation of the start point and the set of pilot nodes (nodes, limits and set-point by period). The *extract_data* file gets the information from the UC: network model, active power program, slack node, parameters of the reactive power control devices and the limits of variables. The terms that make up the objective function are defined in the *extract_data* file, each term can be executed individually for the sensitivity analysis or jointly through the weighted sum, the execution of the parameterization is carried out from the *master*. File *save_solution* saves the optimization results and organizes the information. The optimization results are summarized in a GDX file with the input UC information + the result of the MP-ORPD.

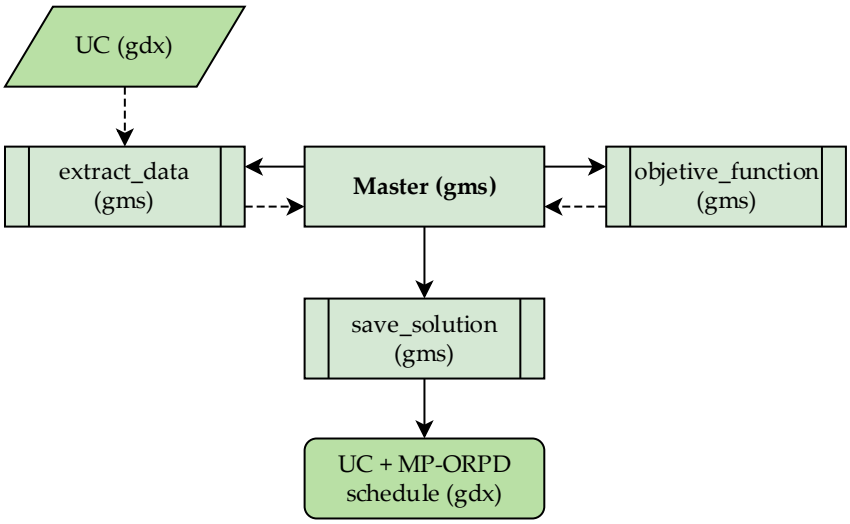

Figure 12. Structure of MP-ORPD solution program in GAMS.

Table A1a–c and Table A2a–c present the full schedule over a 24 h horizon of the MP-OPRD for the IEEE 57- and 118-bus test systems, respectively. Both tables indicate the maneuvers and operational instructions of the control devices. The penalty factors were adjusted as follows: IEEE 57-bus β_1=3E4, β_2=1E-1, and β_3=1E2; IEEE 118-bus β_1=3E5, β_2=1E-2, and β_3=1E2). Table A1a shows that capacitors `C25` and `C53` are always connected because there are few reactive power resources in the IEEE 57-bus test system. Table A2a shows the optimal dispatch of shunt capacitors and reactors. At periods in which the voltage target is low, reactors must be connected and capacitors disconnected; the opposite occurs in periods where the voltage target is high. Additionally, the shunt elements do not show intermittence between continuous periods, which is due to the constraint given by Equation (2). Table A1b and Table A2b present the optimal tap position settings. Table A1c and Table A2c present the optimal voltage setpoints of the generators.

Table A1. Schedule of control variables of the MP-ORPD for IEEE 57-bus system.

(a)

Shnt	Period																							
	1	**2**	**3**	**4**	**5**	**6**	**7**	**8**	**9**	**10**	**11**	**12**	**13**	**14**	**15**	**16**	**17**	**18**	**19**	**20**	**21**	**22**	**23**	**24**
Q_{C18}							10	10	10	10	10	10	10	10	10	10	10	10	10	10	10	10	10	10
Q_{C25}	5.9	5.9	5.9	5.9	5.9	5.9	5.9	5.9	5.9	5.9	5.9	5.9	5.9	5.9	5.9	5.9	5.9	5.9	5.9	5.9	5.9	5.9	5.9	5.9
Q_{C53}	6.3	6.3	6.3	6.3	6.3	6.3	6.3	6.3	6.3	6.3	6.3	6.3	6.3	6.3	6.3	6.3	6.3	6.3	6.3	6.3	6.3	6.3	6.3	6.3

(b)

Trf	Period																							
	1	**2**	**3**	**4**	**5**	**6**	**7**	**8**	**9**	**10**	**11**	**12**	**13**	**14**	**15**	**16**	**17**	**18**	**19**	**20**	**21**	**22**	**23**	**24**
T^1_{4-18}	0.90	0.90	0.90	0.90	0.90	0.90	0.90	0.90	0.90	0.90	0.90	0.90	0.90	0.90	0.90	0.90	0.90	0.90	0.90	0.90	0.90	0.90	0.90	0.90
T^2_{4-18}	0.90	0.90	0.90	0.90	0.90	0.90	0.90	0.90	0.90	0.90	0.90	0.90	0.90	0.90	0.90	0.90	0.90	0.90	0.90	0.90	0.90	0.90	0.90	0.90
T_{7-29}	1.00	1.00	1.00	1.00	1.00	1.00	0.99	0.99	1.00	1.00	1.00	1.00	1.00	1.00	1.00	1.00	1.00	1.00	1.00	1.00	1.00	1.02	1.02	1.00
T_{9-55}	1.01	1.01	1.02	1.02	1.02	1.01	1.08	1.07	1.06	1.10	1.10	1.10	1.06	1.06	1.07	1.07	1.07	1.06	1.10	1.10	1.10	0.97	0.99	1.01
T_{10-51}	0.92	0.92	0.91	0.91	0.91	0.92	0.93	0.94	0.95	0.95	0.95	0.95	0.95	0.95	0.94	0.94	0.94	0.95	0.95	0.95	0.95	0.94	0.94	0.93
T_{11-41}	1.00	1.01	1.01	1.01	1.01	1.00	1.00	0.98	0.97	0.97	0.97	0.97	0.98	0.98	0.98	0.98	0.98	0.98	0.98	0.97	0.98	0.97	0.98	0.99
T_{11-43}	1.00	1.01	1.01	1.01	1.01	1.00	1.00	0.98	0.97	0.97	0.97	0.97	0.97	0.98	0.98	0.98	0.98	0.98	0.98	0.97	0.98	0.97	0.98	0.99
T_{13-49}	0.90	0.90	0.90	0.90	0.90	0.90	0.92	0.93	0.94	0.94	0.94	0.94	0.94	0.94	0.93	0.93	0.93	0.94	0.94	0.94	0.94	0.93	0.93	0.92
T_{14-46}	0.93	0.93	0.92	0.92	0.92	0.93	0.91	0.91	0.90	0.90	0.90	0.90	0.90	0.90	0.90	0.91	0.90	0.90	0.91	0.90	0.91	0.90	0.90	0.91
T_{15-45}	0.98	0.99	1.00	1.03	1.02	0.98	1.02	0.98	0.94	0.94	0.94	0.94	0.95	0.95	0.96	0.97	0.96	0.95	0.95	0.95	0.95	0.93	0.95	0.99
T_{21-20}	1.10	1.10	1.10	1.10	1.10	1.10	1.10	1.10	1.10	1.10	1.10	1.10	1.10	1.10	1.10	1.10	1.10	1.10	1.10	1.10	1.10	1.10	1.10	1.10
T_{24-26}	1.04	1.04	1.04	1.04	1.04	1.04	1.10	1.10	1.10	1.10	1.10	1.10	1.10	1.10	1.10	1.10	1.10	1.10	1.10	1.10	1.10	1.05	1.05	1.05
T_{34-32}	0.97	0.97	0.98	0.98	0.98	0.96	1.05	1.02	0.99	0.99	0.99	0.99	1.00	1.00	1.01	1.01	1.01	1.00	1.00	0.99	1.00	0.97	0.98	0.97
T_{39-57}	0.90	0.90	0.90	0.91	0.91	0.91	0.92	0.96	0.97	0.97	0.98	0.97	0.97	0.97	0.96	0.96	0.96	0.97	0.97	0.97	0.97	0.98	0.96	0.96
T_{40-56}	0.90	0.90	0.90	0.90	0.90	0.90	0.90	0.92	0.94	0.95	0.95	0.95	0.94	0.94	0.93	0.93	0.93	0.94	0.94	0.95	0.94	0.95	0.93	0.91

(c)

Gen	Period																							
	1	**2**	**3**	**4**	**5**	**6**	**7**	**8**	**9**	**10**	**11**	**12**	**13**	**14**	**15**	**16**	**17**	**18**	**19**	**20**	**21**	**22**	**23**	**24**
V_{G1}	0.964	0.963	0.962	0.961	0.962	0.964	1.003	1.003	1.004	1.024	1.024	1.024	1.004	1.004	1.003	1.003	1.003	1.004	1.024	1.024	1.024	0.974	0.973	0.973
V_{G2}	0.956	0.956	0.955	0.955	0.955	0.956	0.995	0.996	0.999	1.019	1.019	1.019	0.999	0.998	0.997	0.997	0.997	0.998	1.018	1.019	1.018	0.968	0.967	0.965
V_{G3}	0.944	0.944	0.944	0.944	0.944	0.944	0.984	0.985	0.986	1.007	1.007	1.007	0.986	0.986	0.985	0.985	0.985	0.986	1.006	1.006	1.006	0.955	0.955	0.954

V_{G6}	0.938	0.938	0.937	0.937	0.937	0.939	0.975	0.984	0.994	1.017	1.018	1.017	0.992	0.991	0.989	0.988	0.989	0.991	1.013	1.016	1.013	0.966	0.96	0.949
V_{G8}	0.947	0.947	0.947	0.947	0.947	0.948	0.984	0.99	0.999	1.02	1.021	1.02	0.997	0.996	0.994	0.992	0.994	0.996	1.018	1.019	1.018	0.969	0.966	0.957
V_{G9}	0.933	0.934	0.934	0.935	0.935	0.933	0.972	0.974	0.976	0.998	0.998	0.998	0.975	0.975	0.975	0.974	0.975	0.975	0.997	0.997	0.997	0.945	0.944	0.941
V_{G12}	0.944	0.944	0.944	0.945	0.945	0.944	0.985	0.985	0.984	1.003	1.003	1.003	0.984	0.984	0.984	0.984	0.984	0.984	1.004	1.003	1.004	0.954	0.954	0.955

Table A2. Schedule of control variables of the MP-ORPD for IEEE 118-bus system.

(a)

Shnt	**Period**																							
	1	**2**	**3**	**4**	**5**	**6**	**7**	**8**	**9**	**10**	**11**	**12**	**13**	**14**	**15**	**16**	**17**	**18**	**19**	**20**	**21**	**22**	**23**	**24**
Q_{L5}	-40	-40	-40	-40	-40	-40	-40	-40	-40				-40	-40	-40	-40	-40	-40				-40	-40	-40
Q_{C34}								14	14	14	14	14	14	14	14	14	14	14	14	14	14	14	14	
Q_{L37}	-25	-25	-25	-25	-25	-25	-25																-25	-25
Q_{C44}	10	10	10	10	10	10	10	10	10	10	10	10	10	10	10	10	10	10	10	10	10	10	10	10
Q_{C45}	10	10	10	10	10	10	10	10	10	10	10	10	10	10	10	10	10	10	10	10	10	10	10	10
Q_{C46}								10	10	10	10	10	10	10	10	10	10	10	10	10	10	10		
Q_{C48}	15	15	15	15	15	15	15	15	15	15	15	15	15	15	15	15	15	15	15	15	15	15	15	15
Q_{C74}									12	12	12	12	12	12	12	12	12	12	12	12	12	12		
Q_{C79}								20	20	20	20	20	20	20	20	20	20	20	20	20	20	20		
Q_{C82}								20	20	20	20	20	20	20	20	20	20	20	20	20	20	20	20	
Q_{C83}							10	10	10	10	10	10	10	10	10	10	10	10	10	10	10	10	10	10
Q_{C105}	20	20	20	20	20	20	20	20	20	20	20	20	20	20	20	20	20	20	20	20	20	20	20	20
Q_{C107}	6	6	6	6	6	6	6	6	6	6	6	6	6	6	6	6	6	6	6	6	6	6	6	6
Q_{C110}	6	6	6	6	6	6	6	6	6	6	6	6	6	6	6	6	6	6	6	6	6	6	6	6

(b)

Trf	**Period**																							
	1	**2**	**3**	**4**	**5**	**6**	**7**	**8**	**9**	**10**	**11**	**12**	**13**	**14**	**15**	**16**	**17**	**18**	**19**	**20**	**21**	**22**	**23**	**24**
T_{8-5}	0.98	0.98	0.98	0.98	0.98	0.98	0.98	0.98	0.98	0.93	0.93	0.93	0.98	0.98	0.98	0.98	0.98	0.98	0.93	0.93	0.93	0.98	0.98	0.98
T_{26-25}	0.90	0.90	0.90	0.90	0.90	0.90	0.90	0.92	0.93	1.00	1.00	1.00	0.93	0.93	0.93	0.93	0.93	0.93	1.00	1.00	1.00	0.93	0.92	0.90
T_{30-17}	0.93	0.93	0.93	0.93	0.93	0.93	0.93	0.94	0.95	0.98	0.99	0.98	0.95	0.95	0.94	0.94	0.94	0.95	0.98	0.98	0.98	0.95	0.94	0.93
T_{38-37}	0.93	0.93	0.93	0.93	0.93	0.93	0.93	0.96	0.97	1.00	1.00	1.00	0.96	0.96	0.96	0.96	0.96	0.96	1.00	1.00	1.00	0.96	0.94	0.93
T_{63-59}	1.03	1.03	1.03	1.04	1.03	1.01	1.00	0.99	0.99	0.98	0.98	0.98	0.99	0.99	0.99	0.99	0.99	0.99	0.98	0.98	0.98	0.99	1.00	1.00
T_{64-61}	0.90	0.90	0.90	0.90	0.90	0.95	0.96	0.95	0.96	0.96	0.96	0.96	0.96	0.95	0.95	0.95	0.95	0.95	0.96	0.96	0.96	0.95	0.96	0.96

T_{65-66}	0.91	0.91	0.90	0.90	0.90	0.90	0.90	0.91	0.92	0.93	0.93	0.93	0.92	0.92	0.92	0.92	0.92	0.92	0.93	0.93	0.93	0.92	0.91	0.90
T_{68-69}	0.93	0.93	0.93	0.93	0.93	0.93	0.94	0.95	0.95	0.96	0.96	0.96	0.95	0.95	0.95	0.95	0.95	0.95	0.96	0.96	0.96	0.95	0.94	0.93
T_{81-80}	0.90	0.90	0.90	0.90	0.90	0.90	0.90	0.90	0.90	0.91	0.91	0.91	0.90	0.90	0.90	0.90	0.90	0.90	0.91	0.91	0.91	0.90	0.90	0.90

(c)

Gen	Period																							
	1	**2**	**3**	**4**	**5**	**6**	**7**	**8**	**9**	**10**	**11**	**12**	**13**	**14**	**15**	**16**	**17**	**18**	**19**	**20**	**21**	**22**	**23**	**24**
V_{G1}	0.965	0.965	0.965	0.965	0.965	0.965	0.973	0.971	0.971	0.983	0.983	0.983	0.971	0.971	0.971	0.970	0.971	0.971	0.983	0.983	0.983	0.964	0.966	0.967
V_{G4}	0.992	0.992	0.992	0.992	0.992	0.992	1.001	1.001	1.001	1.042	1.042	1.042	1.001	1.001	1.001	1.001	1.001	1.001	1.042	1.042	1.042	0.995	0.995	0.995
V_{G6}	0.980	0.980	0.980	0.980	0.980	0.981	0.989	0.989	0.989	1.011	1.011	1.011	0.989	0.989	0.989	0.989	0.989	0.989	1.011	1.011	1.011	0.983	0.983	0.983
V_{G8}	1.006	1.006	1.006	1.006	1.006	1.006	1.014	1.014	1.014	1.021	1.021	1.021	1.014	1.014	1.014	1.014	1.014	1.014	1.021	1.021	1.021	1.008	1.008	1.008
V_{G10}	1.080	1.080	1.080	1.079	1.079	1.080	1.089	1.087	1.086	1.099	1.099	1.099	1.086	1.086	1.086	1.086	1.086	1.086	1.099	1.099	1.099	1.080	1.081	1.083
V_{G12}	0.978	0.978	0.978	0.978	0.978	0.978	0.986	0.985	0.984	0.999	0.999	0.999	0.984	0.985	0.985	0.985	0.985	0.985	0.999	0.999	0.999	0.979	0.979	0.980
V_{G15}	0.967	0.968	0.968	0.968	0.968	0.967	0.975	0.973	0.973	0.981	0.981	0.981	0.973	0.973	0.972	0.972	0.972	0.973	0.981	0.981	0.981	0.966	0.968	0.969
V_{G18}	0.964	0.964	0.964	0.964	0.964	0.964	0.971	0.970	0.970	0.977	0.977	0.977	0.970	0.970	0.969	0.969	0.969	0.970	0.977	0.977	0.977	0.964	0.965	0.965
V_{G19}	0.962	0.962	0.962	0.963	0.962	0.961	0.969	0.967	0.967	0.975	0.975	0.975	0.967	0.967	0.967	0.967	0.967	0.967	0.975	0.975	0.975	0.961	0.962	0.963
V_{G24}	0.986	0.986	0.986	0.985	0.986	0.986	0.995	0.998	0.999	1.008	1.008	1.008	0.998	0.998	0.998	0.998	0.998	0.998	1.008	1.008	1.008	0.993	0.992	0.989
V_{G25}	1.023	1.023	1.022	1.022	1.022	1.023	1.032	1.033	1.034	1.035	1.035	1.035	1.034	1.034	1.034	1.034	1.034	1.034	1.034	1.034	1.034	1.028	1.026	1.026
V_{G26}	0.938	0.938	0.937	0.937	0.937	0.938	0.950	0.969	0.979	1.042	1.043	1.042	0.977	0.976	0.975	0.973	0.975	0.976	1.040	1.042	1.040	0.971	0.960	0.942
V_{G27}	0.957	0.957	0.957	0.956	0.956	0.957	0.964	0.964	0.963	0.970	0.970	0.970	0.963	0.963	0.964	0.964	0.964	0.963	0.970	0.970	0.970	0.958	0.958	0.958
V_{G31}	0.945	0.945	0.945	0.945	0.945	0.945	0.953	0.953	0.952	0.959	0.959	0.959	0.952	0.952	0.952	0.953	0.952	0.952	0.960	0.959	0.960	0.947	0.947	0.947
V_{G32}	0.955	0.955	0.955	0.955	0.955	0.955	0.963	0.963	0.963	0.970	0.970	0.970	0.963	0.963	0.963	0.963	0.963	0.963	0.970	0.970	0.970	0.957	0.957	0.957
V_{G34}	0.979	0.979	0.979	0.979	0.979	0.979	0.987	0.988	0.987	0.995	0.995	0.995	0.987	0.987	0.987	0.987	0.987	0.987	0.995	0.995	0.995	0.981	0.982	0.981
V_{G36}	0.974	0.974	0.974	0.975	0.974	0.974	0.982	0.983	0.982	0.990	0.990	0.990	0.982	0.982	0.982	0.983	0.982	0.982	0.990	0.990	0.990	0.977	0.977	0.976
V_{G40}	0.961	0.962	0.962	0.962	0.962	0.961	0.967	0.967	0.973	0.983	0.983	0.983	0.973	0.972	0.971	0.970	0.971	0.972	0.982	0.982	0.982	0.966	0.960	0.962
V_{G42}	0.972	0.973	0.973	0.973	0.973	0.972	0.979	0.977	0.985	0.995	0.995	0.995	0.984	0.984	0.983	0.981	0.983	0.984	0.994	0.995	0.994	0.977	0.971	0.973
V_{G46}	0.997	0.997	0.997	0.997	0.997	0.997	1.005	1.006	1.006	1.013	1.013	1.013	1.006	1.006	1.006	1.006	1.006	1.006	1.013	1.013	1.013	1.000	1.000	0.999
V_{G49}	1.010	1.010	1.010	1.011	1.011	1.010	1.018	1.017	1.017	1.024	1.024	1.024	1.017	1.017	1.017	1.017	1.017	1.017	1.024	1.024	1.024	1.011	1.011	1.012
V_{G54}	0.948	0.948	0.948	0.948	0.948	0.948	0.956	0.956	0.956	0.962	0.962	0.962	0.956	0.956	0.956	0.956	0.956	0.956	0.962	0.962	0.962	0.950	0.950	0.950
V_{G55}	0.944	0.944	0.944	0.944	0.944	0.944	0.952	0.953	0.953	0.960	0.960	0.960	0.953	0.953	0.953	0.953	0.953	0.953	0.960	0.960	0.960	0.947	0.947	0.946
V_{G56}	0.946	0.946	0.946	0.946	0.946	0.947	0.955	0.955	0.955	0.962	0.962	0.962	0.955	0.955	0.955	0.955	0.955	0.955	0.962	0.962	0.962	0.949	0.949	0.949
V_{G59}	0.948	0.948	0.947	0.947	0.947	0.950	0.960	0.965	0.964	0.974	0.974	0.974	0.964	0.964	0.965	0.966	0.965	0.964	0.975	0.974	0.975	0.959	0.957	0.953
V_{G61}	1.032	1.032	1.031	1.030	1.031	1.001	1.007	1.015	1.016	1.025	1.025	1.025	1.016	1.016	1.016	1.017	1.016	1.016	1.025	1.025	1.025	1.011	1.006	0.999
V_{G62}	1.029	1.028	1.028	1.027	1.027	1.004	1.010	1.017	1.017	1.025	1.025	1.025	1.017	1.017	1.017	1.018	1.017	1.017	1.025	1.025	1.025	1.012	1.008	1.003
V_{G65}	0.962	0.962	0.961	0.960	0.961	0.964	0.975	0.984	0.989	1.005	1.006	1.005	0.988	0.988	0.987	0.987	0.987	0.988	1.003	1.005	1.003	0.982	0.974	0.968

V_{G66}	1.043	1.043	1.043	1.043	1.043	1.043	1.051	1.052	1.052	1.059	1.059	1.059	1.052	1.052	1.051	1.051	1.051	1.052	1.058	1.059	1.058	1.046	1.045	1.045
V_{G69}	1.025	1.025	1.025	1.025	1.025	1.025	1.033	1.034	1.034	1.041	1.041	1.041	1.034	1.034	1.034	1.034	1.034	1.034	1.041	1.041	1.041	1.028	1.028	1.027
V_{G70}	0.975	0.975	0.976	0.976	0.976	0.975	0.983	0.983	0.983	0.991	0.991	0.991	0.983	0.983	0.983	0.983	0.983	0.983	0.991	0.991	0.991	0.977	0.977	0.977
V_{G72}	0.973	0.972	0.971	0.969	0.970	0.974	0.984	0.990	0.992	1.003	1.003	1.003	0.991	0.991	0.991	0.990	0.991	0.991	1.003	1.003	1.003	0.985	0.983	0.978
V_{G73}	0.968	0.967	0.966	0.964	0.965	0.969	0.979	0.984	0.984	0.991	0.991	0.991	0.984	0.984	0.983	0.983	0.983	0.984	0.991	0.991	0.991	0.978	0.976	0.973
V_{G74}	0.961	0.962	0.963	0.964	0.964	0.960	0.966	0.962	0.966	0.973	0.973	0.973	0.965	0.965	0.965	0.966	0.965	0.965	0.973	0.973	0.973	0.959	0.957	0.960
V_{G76}	0.953	0.954	0.955	0.957	0.956	0.951	0.955	0.949	0.949	0.957	0.957	0.957	0.949	0.948	0.948	0.949	0.948	0.948	0.956	0.957	0.956	0.942	0.945	0.949
V_{G77}	1.002	1.002	1.002	1.002	1.002	1.001	1.009	1.008	1.007	1.014	1.014	1.014	1.007	1.008	1.008	1.008	1.008	1.008	1.014	1.014	1.014	1.002	1.002	1.003
V_{G80}	1.027	1.027	1.026	1.026	1.026	1.027	1.036	1.037	1.037	1.044	1.045	1.044	1.037	1.037	1.037	1.037	1.037	1.037	1.044	1.044	1.044	1.031	1.030	1.030
V_{G85}	1.011	1.010	1.009	1.007	1.008	1.012	1.025	1.018	1.020	1.025	1.026	1.025	1.019	1.019	1.018	1.017	1.018	1.019	1.023	1.024	1.023	1.013	1.021	1.019
V_{G87}	1.013	1.011	1.006	1.002	1.004	1.017	1.035	1.035	1.046	1.053	1.054	1.053	1.043	1.041	1.039	1.036	1.039	1.041	1.048	1.051	1.048	1.035	1.038	1.027
V_{G89}	1.029	1.028	1.026	1.024	1.025	1.030	1.042	1.032	1.036	1.041	1.042	1.041	1.035	1.034	1.033	1.032	1.033	1.034	1.039	1.040	1.039	1.028	1.036	1.035
V_{G90}	1.007	1.006	1.004	1.003	1.004	1.008	1.017	1.003	1.004	1.008	1.009	1.008	1.003	1.003	1.002	1.001	1.002	1.003	1.006	1.007	1.006	0.997	1.009	1.011
V_{G91}	1.014	1.013	1.012	1.010	1.011	1.016	1.026	1.014	1.018	1.022	1.023	1.022	1.016	1.015	1.014	1.013	1.014	1.015	1.020	1.021	1.020	1.010	1.019	1.020
V_{G92}	1.021	1.021	1.019	1.018	1.019	1.022	1.032	1.020	1.024	1.029	1.029	1.029	1.022	1.022	1.021	1.020	1.021	1.022	1.027	1.028	1.027	1.016	1.025	1.026
V_{G99}	1.028	1.028	1.027	1.026	1.027	1.029	1.037	1.028	1.035	1.042	1.043	1.042	1.033	1.032	1.031	1.029	1.031	1.032	1.039	1.041	1.039	1.026	1.029	1.031
V_{G100}	1.025	1.025	1.024	1.023	1.024	1.026	1.033	1.021	1.029	1.036	1.037	1.036	1.027	1.025	1.024	1.022	1.024	1.025	1.032	1.034	1.032	1.019	1.023	1.027
V_{G103}	1.022	1.021	1.020	1.019	1.020	1.022	1.028	1.012	1.025	1.033	1.035	1.033	1.022	1.020	1.017	1.014	1.017	1.020	1.027	1.031	1.027	1.013	1.016	1.022
V_{G104}	1.016	1.016	1.015	1.014	1.015	1.017	1.021	1.002	1.016	1.024	1.026	1.024	1.012	1.010	1.007	1.004	1.007	1.010	1.017	1.021	1.017	1.003	1.007	1.016
V_{G105}	1.018	1.017	1.016	1.016	1.016	1.018	1.022	1.002	1.017	1.025	1.028	1.025	1.013	1.011	1.008	1.004	1.008	1.011	1.019	1.023	1.019	1.004	1.008	1.017
V_{G107}	1.016	1.015	1.015	1.014	1.014	1.016	1.019	0.997	1.019	1.028	1.031	1.028	1.014	1.011	1.006	1.001	1.006	1.011	1.020	1.026	1.020	1.002	1.004	1.014
V_{G110}	1.015	1.014	1.013	1.012	1.012	1.016	1.020	1.003	1.024	1.034	1.037	1.034	1.019	1.016	1.012	1.007	1.012	1.016	1.025	1.031	1.025	1.008	1.007	1.015
V_{G111}	1.025	1.024	1.022	1.020	1.021	1.027	1.033	1.019	1.042	1.051	1.055	1.051	1.036	1.033	1.028	1.023	1.028	1.033	1.042	1.048	1.042	1.025	1.022	1.027
V_{G112}	1.005	1.004	1.003	1.002	1.002	1.005	1.009	0.993	1.019	1.029	1.032	1.029	1.012	1.009	1.004	0.998	1.004	1.009	1.019	1.025	1.019	1.000	0.994	1.004
V_{G113}	0.980	0.980	0.980	0.979	0.979	0.980	0.989	0.990	0.991	0.998	0.998	0.998	0.991	0.991	0.991	0.991	0.991	0.991	0.998	0.998	0.998	0.985	0.984	0.983
V_{G116}	0.963	0.962	0.961	0.960	0.961	0.964	0.975	0.983	0.989	1.004	1.005	1.004	0.987	0.987	0.986	0.986	0.986	0.987	1.002	1.003	1.002	0.981	0.974	0.968

References

1. Hassan, M.H.; Kamel, S.; El-Dabah, M.A.; Khurshaid, T.; Dominguez-Garcia, J.L. Optimal Reactive Power Dispatch with Time-Varying Demand and Renewable Energy Uncertainty Using Rao-3 Algorithm. *IEEE Access* **2021**, *9*, 23264–23283. 10.1109/ACCESS.2021.3056423.
2. Sharma, A.; Jain, S.K. Day-ahead optimal reactive power ancillary service procurement under dynamic multi-objective framework in wind integrated deregulated power system. *Energy* **2021**, *223*, 120028. 10.1016/j.energy.2021.120028.
3. Muhammad, Y.; Khan, R.; Raja, M.A.Z.; Ullah, F.; Chaudhary, N.I.; He, Y. Solution of optimal reactive power dispatch with FACTS devices: A survey. *Energy Reports* **2020**, *6*, 2211–2229. 10.1016/J.EGYR.2020.07.030.
4. Sun, H.; Guo, Q.; Zhang, B.; Wu, W.; Wang, B. An adaptive zone-division-based automatic voltage control system with applications in China. *IEEE Trans. Power Syst.* **2013**, *28*, 1816–1828. 10.1109/TPWRS.2012.2228013.
5. Guo, Q.; Sun, H.; Tong, J.; Zhang, M.; Wang, B.; Zhang, B. Study of system-wide automatic voltage control on PJM system. *IEEE PES Gen. Meet. PES 2010* **2010**. 10.1109/PES.2010.5589635.
6. Corsi, S. Voltage control and protection in electrical power systems: From system components to wide-area control. *Volt. Control Prot. Electr. Power Syst. From Syst. Components to Wide-Area Control* **2015**, 1–557. 10.1007/978-1-4471-6636-8.
7. Corsi, S.; Pozzi, M.; Sabelli, C.; Serrani, A. The coordinated automatic voltage control of the Italian transmission grid - Part I: Reasons of the choice and overview of the consolidated hierarchical system. *IEEE Trans. Power Syst.* **2004**, *19*, 1723–1732. 10.1109/TPWRS.2004.836185.
8. Decompositions, O.C.; Rabiee, A.; Member, S.; Parniani, M.; Member, S. Voltage Security Constrained Multi-Period Optimal Reactive Power Flow Using Benders. *IEEE Trans. Power Syst.* **2013**, *28*, 696–708. 10.1109/TPWRS.2012.2211085.
9. Zhang, Y.J.; Ren, Z. Optimal reactive power dispatch considering costs of adjusting the control devices. *IEEE Trans. Power Syst.* **2005**, *20*, 1349–1356. 10.1109/TPWRS.2005.851920.
10. Li, Y.; Cao, Y.; Liu, Z.; Liu, Y.; Jiang, Q. Dynamic optimal reactive power dispatch based on parallel particle swarm optimization algorithm. *Comput. Math. with Appl.* **2009**, *57*, 1835–1842. 10.1016/j.camwa.2008.10.049.
11. Gómez Bedoya, D.A. Metodología para el Análisis de Estabilidad de Tensión Mediante la División de Redes en Áreas de Control. Licentiate Thesis, Facultad de Ingenierías Eléctrica, Electrónica, Física y Ciencias de la Computación, Universidad Tecnológica de Pereira, Pereira, Colombia, **2014**.
12. Bingane, C.; Anjos, M.F.; Le Digabel, S. Tight-and-Cheap Conic Relaxation for the Optimal Reactive Power Dispatch Problem. *IEEE Trans. Power Syst.* **2019**, *34*, 4684–4693. 10.1109/TPWRS.2019.2912889.
13. Villa-Acevedo, W.M.; López-Lezama, J.M.; Valencia-Velásquez, J.A. A Novel Constraint Handling Approach for the Optimal Reactive Power Dispatch Problem. *Energies* **2018**, *11*, 1–23.
14. Constante F., S.G.; Lopez, J.C.; Rider, M.J. Optimal Reactive Power Dispatch with Discrete Controllers Using a Branch-and-Bound Algorithm: A Semidefinite Relaxation Approach. *IEEE Trans. Power Syst.* **2021**. 10.1109/TPWRS.2021.3056637.
15. Masoud Mohseni-Bonab, S.; Rabiee, A. Optimal reactive power dispatch: a review, and a new stochastic voltage stability constrained multi-objective model at the presence of uncertain wind power generation. *IET Gener. Transm. Distrib.* **2017**, *11*, 815–829. 10.1049/iet-gtd.2016.1545.
16. Davoodi, E.; Babaei, E.; Mohammadi-Ivatloo, B.; Rasouli, M. A novel fast semidefinite programming-based approach for optimal reactive power dispatch. *IEEE Trans. Ind. Informatics* **2020**, *16*, 288–298. 10.1109/TII.2019.2918143.

17. Cain, M.B.; O'Neill, R. History of Optimal Power Flow and Formulations. Fed. Energy Regul. Comm., vol. 1, pp. 1–36, **2012**.
18. Babaeinejadsarookolaee, S.; Birchfield, A.; Christie, R.D.; Coffrin, C.; DeMarco, C.; Diao, R.; Ferris, M.; Fliscounakis, S.; Greene, S.; Huang, R.; et al. The Power Grid Library for Benchmarking AC Optimal Power Flow Algorithms. **2019**.
19. Hu, Z.; Wang, X.; Taylor, G. Stochastic optimal reactive power dispatch: Formulation and solution method. *Int. J. Electr. Power Energy Syst.* **2010**, *6*, 615–621. 10.1016/J.IJEPES.2009.11.018.
20. Saddique, M.S.; Bhatti, A.R.; Haroon, S.S.; Sattar, M.K.; Amin, S.; Sajjad, I.A.; ul Haq, S.S.; Awan, A.B.; Rasheed, N. Solution to optimal reactive power dispatch in transmission system using meta-heuristic techniques—Status and technological review. *Electr. Power Syst. Res.* **2020**, *178*. 10.1016/j.epsr.2019.106031.
21. Sharif, S.S.; Taylor, J.H. Dynamic optimal reactive power flow. In Proceedings of the Proceedings of the American Control Conference; IEEE, **1998**; Vol. 6, pp. 3410–3414. 10.1109/ACC.1998.703223.
22. Frank, S.; Steponavice, I.; Rebennack, S. Optimal power flow: A bibliographic survey I Formulations and deterministic methods. *Energy Syst.* **2012**, *3*, 221–258. 10.1007/s12667-012-0056-y.
23. Ebeed, M.; Alhejji, A.; Kamel, S.; Jurado, F. Solving the Optimal Reactive Power Dispatch Using Marine Predators Algorithm Considering the Uncertainties in Load and Wind-Solar Generation Systems. *Energies 2020, Vol. 13, Page 4316* **2020**, *13*, 4316. 10.3390/EN13174316.
24. Belotti, P.; Kirches, C.; Leyffer, S.; Linderoth, J.; Luedtke, J.; Mahajan, A. Mixed-integer nonlinear optimization*†. *Acta Numer.* **2013**, *22*, 1–131. 10.1017/S0962492913000032.
25. Ruiz, M.; Maeght, J.; Marié, A.; Panciatici, P.; Renaud, A. A progressive method to solve large-scale AC optimal power flow with discrete variables and control of the feasibility. *Proc. - 2014 Power Syst. Comput. Conf. PSCC 2014* **2014**. 10.1109/PSCC.2014.7038395.
26. Tinney, W.F.; Bright, J.M.; Demaree, K.D.; Hughes, B.A. Some deficiencies in optimal power flow. *IEEE Trans. Power Syst.* **1988**, *3*, 676–683. 10.1109/59.192922.
27. Zhao, J.; Ju, L.; Dai, Z.; Chen, G. Voltage stability constrained dynamic optimal reactive power flow based on branch-bound and primal–dual interior point method. *Int. J. Electr. Power Energy Syst.* **2015**, *73*, 601–607. 10.1016/J.IJEPES.2015.05.038.
28. Huang, J.; Li, Z.; Wu, Q.H. Fully decentralized multiarea reactive power optimization considering practical regulation constraints of devices. *Int. J. Electr. Power Energy Syst.* **2019**, *105*, 351–364. 10.1016/J.IJEPES.2018.08.045.
29. Zhang, L.; Tang, W.; Liang, J.; Cong, P.; Cai, Y. Coordinated Day-Ahead Reactive Power Dispatch in Distribution Network Based on Real Power Forecast Errors. *IEEE Trans. Power Syst.* **2016**, *31*, 2472–2480. 10.1109/TPWRS.2015.2466435.
30. Mazzini, A.P.; Asada, E.N.; Lage, G.G. Minimisation of active power losses and number of control adjustments in the optimal reactive dispatch problem. *IET Gener. Transm. Distrib.* **2018**, *12*, 2897–2904. 10.1049/IET-GTD.2017.1486.
31. Liu, M.B.; Cañizares, C.A.; Huang, W. Reactive power and voltage control in distribution systems with limited switching operations. *IEEE Trans. Power Syst.* **2009**, *24*, 889–899. 10.1109/TPWRS.2009.2016362.
32. Soman, S.A.; Parthasarathy, K.; Thukaram, D. Curtailed number and reduced controller movement optimization algorithms for real time voltage/reactive power control. *IEEE Trans. Power Syst.* **1994**, *9*, 2035–2041. 10.1109/59.331466.
33. Chen, G.; Liu, L.; Huang, S. Enhanced GSA-based optimization for minimization of power losses in power system. *Math. Probl. Eng.* **2015**, *2015*. 10.1155/2015/527128.
34. Enrique, N.; Ramírez, G. Metodología de gestión de potencia reactiva para mejorar el margen de estabilidad de voltaje en sistemas eléctricos de potencia descentralizados ; Medellín , **2014**.
35. Rabiee, A.; Vanouni, M.; Parniani, M. Optimal reactive power dispatch for improving voltage stability margin using a local voltage stability index. *Energy Convers. Manag.* **2012**, *59*, 66–73. 10.1016/j.enconman.2012.02.017.
36. Gutiérrez, D.; López, J.M.; Villa, W.M. Metaheuristic Techniques Applied to the Optimal Reactive Power Dispatch: A Review. *IEEE Lat. Am. Trans.* **2016**, *14*, 2253–2263. 10.1109/TLA.2016.7530421.

37. Oureilidis, K.; Malamaki, K.-N.; Gallos, K.; Tsitsimelis, A.; Dikaiakos, C.; Gkavanoudis, S.; Cvetkovic, M.; Mauricio, J.M.; Maza Ortega, J.M.; Ramos, J.L.M.; et al. Ancillary Services Market Design in Distribution Networks: Review and Identification of Barriers. *Energies* **2020**, *13*, 917. 10.3390/en13040917.
38. Ferreira, E.C.; Neto, M.S.I.; Asada, E.N. Metaheuristic strategies for solving the Optimal Reactive Power Dispatch with discrete variables. In Proceedings of the 2016 12th IEEE International Conference on Industry Applications, INDUSCON 2016; Institute of Electrical and Electronics Engineers Inc., **2017**. 10.1109/INDUSCON.2016.7874516.
39. ß Kılıç, U.; ßat Ayan, K.; Arifog, ur Optimizing reactive power flow of HVDC systems using genetic algorithm. *Int. J. Electr. Power Energy Syst.* **2014**, *55*, 1–12. 10.1016/j.ijepes.2013.08.006.
40. Mugemanyi, S.; Qu, Z.; Rugema, F.X.; Dong, Y.; Bananeza, C.; Wang, L. Optimal Reactive Power Dispatch Using Chaotic Bat Algorithm. *IEEE Access* **2020**, *8*, 65830–65867. 10.1109/ACCESS.2020.2982988.
41. Ghaljehei, M.; Soltani, Z.; Lin, J.; Gharehpetian, G.B.; Golkar, M.A. Stochastic multi-objective optimal energy and reactive power dispatch considering cost, loading margin and coordinated reactive power reserve management. *Electr. Power Syst. Res.* **2019**, *166*, 163–177. 10.1016/J.EPSR.2018.10.009.
42. Yang, S.; Wang, W.; Liu, C.; Huang, Y. Optimal reactive power dispatch of wind power plant cluster considering static voltage stability for low-carbon power system. *J. Mod. Power Syst. Clean Energy 2015 31* **2015**, *3*, 114–122. 10.1007/S40565-014-0091-X.
43. Lakkaraju, T. Selection of pilot buses for VAR support and voltage stability risk analysis. *Grad. Theses, Diss. Probl. Reports* **2006**. https://doi.org/10.33915/etd.1776.
44. Zhang, W.; Tolbert, L.M. Survey of reactive power planning methods. *2005 IEEE Power Eng. Soc. Gen. Meet.* **2005**, *2*, 1430–1440. 10.1109/PES.2005.1489402.
45. Biskas, P.N.; Ziogos, N.P.; Tellidou, A.; Zoumas, C.E.; Bakirtzis, A.G.; Petridis, V. Comparison of two metaheuristics with mathematical programming methods for the solution of OPF. *IEE Proc. Gener. Transm. Distrib.* **2006**, *153*, 16–24. 10.1049/IP-GTD:20050047.
46. Tang, L.; Ferris, M. *Collection of Power Flow models: Mathematical formulations*; University of Wisconsin: Madison, WI, USA, **2015**.
47. Park, B.; Tang, L.; Ferris, M.C.; Demarco, C.L. Examination of Three Different ACOPF Formulations with Generator Capability Curves. *IEEE Trans. Power Syst.* **2017**, *32*, 2913–2923. 10.1109/TPWRS.2016.2626142.
48. FlameJaguar/MP-ORPD: Multi-Period Optimal Reactive Power Dispatch data files Available online: https://github.com/FlameJaguar/MP-ORPD (accessed on Aug 17, 2021).
49. coin-or/Bonmin: Basic Open-source Nonlinear Mixed INteger programming Available online: https://github.com/coin-or/Bonmin (accessed on Sep 2, 2021).
50. Bussieck, M.; Vigerske, S. MINLP solver software. In: Cochran, J.J., Cox, L.A., Keskinocak, P., Kharoufeh, J.P., Smith, J.C. (eds.) Wiley Encyclopedia of Operations Research and Management Science. Wiley, New York. **2010**.
51. Grigg, C.; Wong, P. The IEEE reliability test system -1996 a report prepared by the reliability test system task force of the application of probability methods subcommittee. *IEEE Trans. Power Syst.* **1999**, *14*, 1010–1020. 10.1109/59.780914.
52. El-Araby, E.-S.E.; Yorino, N. Reactive power reserve management tool for voltage stability enhancement. *IET Gener. Transm. Distrib.* **2018**, *12*, 1879–1888. 10.1049/IET-GTD.2017.1356.
53. *Optimal Power Flow: Comparison with Matpower | NEOS*. (n.d.) Available online: https://neos-guide.org/content/opf-matpower-comparison (accessed on Feb 17, 2022).